NASA Technical Memorandum 107341

Factors Influencing Pitot Probe Centerline Displacement in a Turbulent Supersonic Boundary Layer

Wendy I. Grosser
Lewis Research Center
Cleveland, Ohio

January 1997

National Aeronautics and
Space Administration

Chapter I

Introduction

Pitot tubes are used extensively in fluid flow to measure total pressure for velocity calculations. It is well known, however, that the presence of the pitot probe in shear flow—even in incompressible flow—alters the nature of the flow. The nature of the alteration can be divided into three effects:

1. Reynolds Number Effect: This effect is important when $R_D < 200$ (Reynolds number based on pitot tube diameter).
2. Wall Effect: This effect is only seen when the pitot tube is stationed within two diameters of a solid boundary.
3. Velocity Gradient/Centerline Displacement Effect: This effect is always present, and is caused by two things: (1) the pitot probe deflecting the incoming streamlines and (2) the average pressure across the pitot probe face is not equal to the impact pressure measured at the geometric center of the probe. Figure 1.1 illustrates the centerline displacement effect.

Of these three effects, the centerline displacement effect is the most predominant in high speed boundary layer flow. It has been the goal of previous researchers and is the goal of this paper to understand the nature of the centerline displacement effect in order to compensate for it.

NOMENCLATURE

U.S. Customary Units were employed for the experimental measurements in this study, but the International System of Units (SI) are used to report the results.

C constant in law-of-the-wall equation

C_f coefficient of friction

D external diameter of pitot probe

d internal diameter of pitot probe

M Mach number

p_s static pressure

p_t total pressure

p_{t2} pitot pressure

R_D Reynolds number based on D, $(\rho_e u_e D)/\mu_e$

T_t total temperature

T_s static temperature

U^+ dimensionless velocity (u^*/u_τ)

u local velocity

u_τ frictionless velocity $(\sqrt{\tau_w/\rho})$

u^* Van Driest generalized velocity

y distance from the wall

y^+ dimensionless distance from the wall (yu_τ/u)

Greek

γ ratio of specific heats, $c_p/c_v = 1.4$ for air

Δ centerline offset

δ boundary layer thickness

κ Von Karman constant

μ dynamic viscosity

ν kinematic viscosity

ρ density

τ shear stress

Subscripts

e property evaluated at the boundary layer edge

wall property evaluated at the wall

∞ property evaluated in the free stream

o wind tunnel plenum conditions

1 property evaluated upstream of shock wave

2 property evaluated downstream of shock wave

1.1 LITERATURE REVIEW

The pitot probe centerline displacement effect was first studied by Young & Maas (1936). For their experiment they made multiple pitot traverses behind a symmetrical wing section in a 0.71×0.508 m (2.33×1.67 ft) open return-flow wind tunnel at Cambridge. They ran two airspeeds: 182.9 and 230.1 m/s (60 and 75 ft/s) and used six different-diameter, square-cut pitot probes with an average inside to outside diameter ratio (d/D) of 0.6. From their experiments, Young & Maas discovered that their velocity versus wall height curves were offset from the "true curves" (their true curves were determined using extremely small pitot probes). They theorized that this offset could be viewed as either a ΔU or a Δy. They chose to view their offset as a Δy because theory predicted that the incoming streamlines would bend around the protruding pitot tube and, thus, be offset by a certain Δy. Young & Maas noticed that the effective center of their pitot tubes were displaced from the geometric center towards the region of higher velocity. Denoting this centerline offset Δ,[1] they found that Δ/D (where D is the outside diameter of the pitot tube) was relatively independent of D and was equal to 0.18 when d/D equaled 0.6. Young & Maas then performed a second series of tests to determine the displacement effect due to varying d/D (inner diameter/outer diameter). Three different pitot tubes with d/D = 0.138, 0.35, and 0.73 were used. From these tests Young & Maas created the relation that $\Delta/D = 0.131 + 0.082(d/D)$ for any d.

The next researcher to investigate the centerline displacement effect was F.V. Davies (1952). Davies' experiments were done in a 0.127×0.127 m (5×5 in.) supersonic wind tunnel with $M_\infty = 2.43$. He ran experiments using both a flat plate and a cone, and his flow was laminar for both cases. Davies divided his results into three distinct categories: displacement of the boundary layer velocity profile (variation in slope), distortion of the velocity profile near the free stream, and distortion of the velocity profile near the boundary surface. Unlike Young & Maas, however, Davies found that his profiles were displaced in the direction of lower velocity (an effect he later concluded was due to the fact that his probes were flattened probes and Young & Maas's probes were circular). From his research Davies found an error of $\Delta/D = -0.15$. Davies set a lower limit of d/D = 0.2 on the inner to outer diameter ratio to limit the velocity profile distortion near the free stream.

Livesey (1956) conducted experiments in the turbulent boundary layer of Rolls-Royce's 7×5 ft wind tunnel. His purpose was to select a probe design that would have negligible centerline displacement effects. For his experiments he used a conical nose probe with d/D = 0.7, a conical nose probe with d/D = 0.5 and a hemispherical nose probe with d/D = 0.5 (remember that previous researchers had used square-cut pitot probes). Livesey found that the conical nose pitot probe produced a Δ/D of less than 0.02 while the hemispherical nose produced a Δ/D of 0.10 (compared to Young & Maas's 0.15). From these results, Livesey concluded that the conical nosed pitot probe might be the best probe to use since it appears to have a negligible displacement error. It has, however, since been concluded that conical probes have their limitations in supersonic flow (Bryer & Pankhurst, 1971).

MacMillan performed his well documented and oft-referenced experiments in 1957. His goal was to determine both the centerline offset error and the wall effect error and to combine them into one error or error formula if possible. MacMillan ran his experiments using laminar, low-speed flow conditions in a pipe and on a flat plate with zero pressure gradient. Five circular, square-cut pitot probes with average d/D = 0.6 were traversed across the pipe and through the flat plate boundary layer to measure pressure/velocity versus y. At every y-value the Mach versus D was plotted for each pitot tube and the resulting points were curve-fitted then extrapolated back to zero to determine the Mach at D = 0. These resulting points were plotted as the true curve and each pitot probe error was determined from their offset from this true curve. MacMillan found that when $y/D > 2$ (the probe centerline was located greater than two diameter from the wall, see fig. 1.2), the effective center is displaced towards the region of higher velocity by a constant centerline offset of $\Delta/D = 0.15$ (versus $\Delta/D = 0.18$ for Young & Maas). When $y/D < 2$ then an additional correction—a u/U correction—must be applied. This new correction is solely a function of y/D and MacMillan plotted the resulting curve in what has become a well reproduced curve (fig. 1.3).

P. Davies (1957) conducted subsonic turbulent boundary layer and wake flow using square-cut pitot probes of five various outer diameters. His purpose was to compare the errors of these two types of flow conditions (boundary layer versus wake). For his boundary layer testing, Davies theorized that the worst error would occur with the probe on the wall and thus took data only with each probe touching the wall. Davies found no appreciable error and thus concluded that "the absence of such corrections in the present results may be due to the higher response rate of the manometer system used."

[1]Young & Maas denoted centerline offset by "δ," but here "Δ" is used to avoid confusion with boundary layer thickness also denoted by "δ."

The final and most recent pitot probe centerline displacement research was done by Jerry M. Allen (1972) at Langley Research Center. In his Technical Note, Allen outlined an experiment very similar to MacMillan's, but his probe survey was conducted in a supersonic, turbulent boundary layer (as opposed to an incompressible, turbulent boundary layer). His purpose was to provide experimental data on the pitot-probe displacement in a supersonic turbulent boundary layer and to investigate how different ratios of D/δ (where δ is the boundary layer thickness) affect the boundary layer profile. Allen used probes with D/δ ranging from 0.018 to 0.691 and ran his experiments at $M_\infty = 2$ and a unit $R_\infty = 8\times10^6$ /m. Unlike MacMillan and P. Davis, Allen's Δ/D may be dependent on D and is approximately equal to 0.38 at $D = 0$ (a calculated value). Allen also found that "large" probes distorted the shape of the boundary-layer profile—large being defined as $D/\delta > 0.145$. Figure 1.4 recreates figure 11 in Allen's paper and neatly summarizes previous research on centerline displacement error. Table I summarizes the conditions and results of previous investigators.

1.2 SCOPE OF WORK

The purpose of this research was to continue the investigation of the centerline displacement error for supersonic turbulent boundary layers. Data were collected in three NASA Lewis Research Center Supersonic Wind Tunnels (SWT's): the 10×10 ft SWT, the 1×1 ft SWT and the 15×15 cm SWT. Table II summarizes the Mach numbers, Reynolds numbers, D/δ, and boundary layers of the present experiment. Included in this table are the conditions tested by Allen.

The present study was undertaken to expand upon Allen's supersonic turbulent boundary layer research by considering a wider range of operating conditions. The results of this study, in conjunction with previous research, was to be used to determine what factors influence pitot probe centerline displacement in a supersonic, turbulent boundary layer. The conclusions from this paper will provide valuable insight for researchers involved in supersonic turbulent boundary layer experimentation.

Chapter II

Description of Experiment

2.1 FACILITIES

Research was conducted in three separate NASA Lewis Research Center (LeRC) Supersonic Wind Tunnels: the 10×10 ft SWT, the 15×15 cm SWT, and the 1×1 ft SWT. Details about each facility and their respective tests are given in the following sections. For all facilities, tunnel freestream conditions were measured using combination rakes in the tunnels' plenum.

2.1.1 Description of LeRC 10×10 ft SWT

The NASA LeRC 10 ft x 10 ft Supersonic Wind Tunnel (SWT) is a propulsion tunnel primarily used to conduct supersonic inlet research. The 10×10 ft SWT is capable of producing test section Mach numbers from $M_\infty = 2.0$ to $M_\infty = 3.5$ with Reynolds numbers ranging from approximately 0.98×10^6 to 11.5×10^6/m (0.3×10^6 to 3.5×10^6/ft). The test section is 3.048 m high $\times$ 3.048 m wide $\times$ 12.19 m long ($10 \times 10 \times 40$ ft) and starts approximately 16.7 m (55 ft) downstream of the throat. Figure 2.1 shows a planform view of the entire 10×10 ft SWT loop and figure 2.2 shows an elevation view of the test section.

2.1.2 Description of LeRC 15×15 cm SWT

The 15×15 cm SWT tunnel provides the capability for the development and calibration of instruments at supersonic conditions and for other studies related to high speed research. It has a test section 15 by 15 cm (approximately 0.5×0.5 ft). The facility is an open loop, continuous flow wind tunnel with Mach number variations provided by replaceable fixed-geometry nozzle blocks. Current available Mach numbers are $M_\infty = 2.0$, 2.5 and 3.0, and the Reynolds number can be varied from 6.0×10^6/m to 20×10^6/m. Figure 2.3 shows a sketch of the 15×15 cm SWT.

2.1.3 Description of LeRC 1×1 ft SWT

The 1×1 ft SWT is a continuous flow aerodynamic facility used for inlet testing, shock/boundary layer interactions, and code verification of computational fluid dynamics. The test section measures 0.305 m high by 0.310 m wide by 0.66 m long ($1 \times 1.17 \times 2.17$ ft). The 1×1 ft SWT is capable of producing Mach numbers equal to 1.3, 1.6, 2.0, 2.5, 3.0, 3.5, 4.0, 5.0, 5.5, and 6.0. Reynolds number can be varied from 1.6×10^6/m to 52×10^6/m (0.5×10^6/ft to 16×10^6/ft). Figure 2.4 shows a sketch of the 1×1 ft SWT.

2.2 TEST STATION

2.2.1 10 × 10 ft SWT Test Station

The 10 × 10 ft SWT test section has two sets of sidewall window inserts—one set 1.588 m (5.208 ft) from the beginning of the test section and the other set 4.763 m (15.208 ft) from the beginning of the test section. The centerlines of these windows are 254 mm (10 in.) above the tunnel centerline, and schlieren windows are normally mounted in these inserts. Figure 2.2 shows the window inserts.

For this experiment, one 10 × 10 ft SWT window insert was modified to allow the insertion of a test plate which contained a diamond shaped hole, twelve static taps and two thermocouple plugs (fig. 2.5). The test plate was held in place by a retaining ring and which contained two O-ring seals to ensure proper sealing (fig. 2.6).

The probe-tip survey station was located approximately 17.6 m (57.8 ft) downstream of the throat. The boundary layer at this point was turbulent and was 205 mm (8.06 in.) and 224 mm (8.83 in.) thick for Mach = 2.0 and Mach = 2.5, respectively.

Outside the test section an aluminum table was mounted to the test plate frame and the test hardware was mounted to this table. Figure 2.7 shows a photograph of the window insert, the schlieren window, the plate insert, and the test table. Figure 2.8 shows a close-up of the test table and the test hardware for the 10 × 10 ft SWT test.

2.2.2 15 × 15 cm SWT Test Station

The 15 × 15 cm SWT test station consisted of a removable side plate that had a through hole for the probe and a static tap to read the local static pressure. The probe-tip survey station was located approximately 870 mm downstream of the tunnel throat. The boundary layer at that point was turbulent and was equal to 130 mm.

2.2.3 1 × 1 ft SWT Test Station

The 1 × 1 ft SWT test station also consisted of a removable side plate that had a through hole for the probe and static taps for local static pressure. The probe-tip survey station was located approximately 195 mm downstream of the tunnel throat. The boundary layer at the test station varied from 25.5 to 29.3 mm, depending on the Mach number and Reynolds number that was set. Refer back to table II for boundary layer values at each condition.

2.3 INSTRUMENTATION

2.3.1 10 × 10 ft SWT Instrumentation

The 10 × 10 ft SWT boundary layer was surveyed with five round pitot probes. Four relatively large diameter probes—0.32, 0.64, 0.95, and 1.27 cm (0.1875, 0.25, 0.375, and 0.5 in. respectively)—and one small diameter probe, 0.051 cm (0.02), were used for the survey. A photograph of the probes is shown in figures 2.9, 2.10 and 2.11. The tips of all probes were beveled for yaw insensitivity,[2] and the average ratio of inside diameter to outside diameter was 0.6. The bases of the four largest probes were threaded and had O-rings for sealing. These probes were threaded into a separate adapter piece that was mounted in the strut (fig. 2.12). Figure 2.13 shows the 1.27 cm probe installed in the strut.

The fifth and smallest diameter probe was brazed to a separate adapter and bent toward the wall to ensure that the probe tip touched the wall before the rest of the probe. Figure 2.14 shows the 0.051 cm diameter probe installed in the strut.

The strut, shown in figure 2.15, was 660.4 mm (26 in.) long and was fabricated from stainless steel. 406.4 mm (16 in.) of the strut had a diamond cross sectional area and the remaining 254 mm (10 in.) had a rectangular cross section. A 6.35 mm (0.25 in.) diameter hole was drilled from the tip of the probe through to a slot in the rectangular section, and the top of the strut was milled out to allow the mounting of the adapter piece.

[2]It has been well documented (Chue, 1972) that a pitot probe with a 15° bevel is insenitive to yaw angles of ±15°.

The adapter piece had a 3.18 mm O.D. tube (0.125 in.) brazed to its base to produce a hard-lined route from the pitot tube through the strut. The adapter was fastened to the strut with a #4 screw and RTV silicon epoxy was used to seal around the adapter/strut interface to prevent leakage.

The base of the pitot probe strut was bolted to a linear positioner table outside the test section. The table had a range of 304.8 mm (12 in.) and an accuracy of ±0.25 mm (±0.010 in.), or ±0.08 percent of full scale. The table was driven by a compumotor and the position of the table was read using a linear pot, and with an encoder.

The clearance between the strut and the diamond-shaped hole in the tunnel sidewall was 0.25 mm (0.010 in.) total. To prevent leakage and to aide in alignment, a split-half brass sleeve was bolted to the sidewall test plate around the strut. The sleeve-to-sidewall plate interface had an O-ring and the sleeve-to-strut interface had O-rings. Vacuum grease applied to the strut helped the strut move easily through the sleeve.

Pitot-probe pressure was read using the 10×10 ft SWT facility Escort D^+ system, a minicomputer-based, real-time, data acquisition system. The accuracy of this system for a 103.42 ka (15 psi) module is 0.07 percent of full scale. Static pressures were measured using Setra 370's which are more accurate at low pressures (average error of 0.048 ka or 0.007 psia). All data were stored on a mainframe computer in the NASA-Lewis's Research Analysis Center for reduction purposes.

2.3.2 15 × 15 cm SWT and 1 × 1 ft SWT Instrumentation

Both the 15×15 cm SWT boundary layer and the 1×1 ft SWT boundary layer were surveyed with five round pitot probes. Four "experimental" probes—0.051, 0.091, 0.147, and 0.210 cm (0.02, 0.036, 0.058, and 0.083 in. respectively)—and one boundary layer survey probe, 0.036 cm (0.014). A photograph of one pitot probe is shown in figure 2.16.

For both facilities, the pitot probe support tube was inserted through a grommeted hole in the sidewall then clamped into a Newport actuator. The grommet allowed easy movement while preventing leakage.

Pitot probe pressures were read using the facility Escort D^+ system, the same type of system that exists in the 10×10 ft SWT facility. All data were stored on a mainframe computer in the NASA LeRC Research Analysis Center for reduction purposes.

2.3.3 Probe Position Zeroing Technique

In the 10×10 ft SWT the pitot probe zero position was established by running the probe strut to the wall and using shim gages to verify that the probe tip was touching the wall. During testing, the probe was moved in 1.27 mm (0.05 in.) increments until the total pressure read by the probe changed (to account for any "spring" in the probe). The encoder value at this point was recorded by the computer and all subsequent values had this "zero" position value subtracted from them.

In the 15×15 cm and the 1×1 ft SWTs the probe struts were retracted until an audible alarm sounded—this alarm was triggered by the stainless steel probe touching the stainless steel tunnel wall and completing an electrical circuit. Visual inspection (and a bit of probe manipulation) verified that the probe tip was slightly bent and thus touched first. With the probe tip on the wall, the computer program responsible for probe positioning was set to zero and the probe was actuated a couple of times to verify that the zero position was repeatable.

2.4 Test and Procedures

The tests were conducted in three separate NASA Lewis Research Supersonic Wind Tunnels: the 10×10 ft SWT, the 15×15 cm SWT, and the 1×1 ft SWT. Freestream conditions for each facility are given in table III. Prior to testing, the pitot tubes were leak checked and the zero positions of the probes were calibrated—the probes were fully retracted and visual inspection verified that the tip was on the wall. In the 15×15 cm SWT and 1×1 ft SWT facilities, the probe strut was given a small electrical charge such that when the probe tip touched the wall of the tunnel a circuit was completed and an audible alarm sounded.

In the 10×10 ft SWT, the linear positioning table was controlled using a fluke controller—all positions were fed into the computer prior to testing, and the controller stepped through the program when the "Enter" key was pressed on the keyboard. After each position change, the static pressures beneath the probe tip were allowed to settle before the data point was recorded to Escort (the pitot pressure settled much faster than the static pressures).

In the 15×15 cm SWT and the 1×1 ft SWT the probe positions were controlled using a PACS system and a Newport actuator, where, again, the positions were preprogramed and the whole matrix was automated. Through trial and error, ample time was allowed at each y-position for the pressures to settle out before the data point was recorded.

Chapter III

Data Reduction

All values recorded during testing were loaded into a PC based program called PV-WAVE Personal Edition, created by Visual Numerics. Multiple programs were written to reduce and plot the data using the methods detailed below.

3.1 EDGE MACH NUMBER

The boundary layer edge Mach number for all the facilities was calculated from the implicit isentropic relation (eq. (8) of Bryer and Pankhurst, 1971):

$$\frac{p_{t_2,e}}{p_{t,o}} = \left(\frac{6M_e^2}{M_e^2+5}\right)^{7/2}\left(\frac{6}{7M_e^2-1}\right)^{5/2} \tag{1}$$

where $p_{t2,e}$ is the pitot pressure measured in the freestream of the wind tunnel and $p_{t,o}$ is the wind tunnel stagnation pressure. By calculating the Mach number by this equation, it is assumed that there is a negligible loss in stagnation pressure in the wind tunnel core flow between the plenum and the measurement station. This method for determining the edge Mach number is an alternative to the more common procedure of using the freesteam pitot and local wall static pressures to calculate edge Mach number via the Rayleigh Pitot tube equation. The reason for using equation (1) was the 15×15 cm SWT facility did not have wall static pressure taps at the measurement station. For consistency, the data for the two other facilities were reduced in the same manner.

3.2 STATIC PRESSURE

For the purposes of data reduction, the static pressure was assumed to be constant across the boundary layer and was calculated from the isentropic relation:

$$p_s = p_{t,o}\left(1+\frac{\gamma-1}{2}M_e^2\right)^{-\gamma/\gamma-1} \tag{2}$$

For the two facilities (the 10×10 ft SWT and the 1×1 ft SWT) which had wall static pressure taps at the measurement station, the calculated and measured values were compared and found to agree within ±0.5 percent.

3.3 LOCAL MACH NUMBER

Two formulas were used to calculate the local Mach number using the static pressure and the pitot pressure:

$$\frac{p_{t_2}}{p_s} = \left(1 + \frac{\gamma - 1}{2} M^2\right)^{\gamma/\gamma - 1} \tag{3}$$

for pressure ratios less than 1.893 (Mach < 1.0) and

$$\frac{p_{t_2}}{p_s} = \left(\frac{\gamma + 1}{2} M^2\right)^{\gamma/\gamma - 1} \left(\frac{\gamma + 1}{2\gamma M^2 - \gamma + 1}\right)^{1/\gamma - 1} \tag{4}$$

for pressure ratios greater than 1.893 (M > 1.0). Equation (4) is the Rayleigh pitot formula from Breyer and Pankhurst (1971).

The boundary layer edge Mach numbers, M_e, were chosen to be the freestream Mach number.

3.4 LOCAL VELOCITY

Knowing the local Mach number and the edge Mach number, the local velocity ratios were then calculated from the following formula:

$$\frac{u}{u_e} = \frac{M}{M_e} \sqrt{\frac{T_{s_{wall}}}{T_{t_\infty}}} \sqrt{\frac{T_{t_e}}{T_{s_e}}} \sqrt{\frac{T_{t_\infty}}{T_{t_e}}} \tag{5}$$

but

$$\sqrt{\frac{T_{t_\infty}}{T_{t_e}}} = 1.0 \tag{6}$$

and, using a recovery factor of 0.89 and assuming adiabatic conditions:

$$T_{s_{wall}} = 0.89\left(T_{te} - T_{se}\right) + T_{se} \tag{7}$$

$$\frac{T_{t_e}}{T_{s_e}} = 1 + \frac{\gamma - 1}{2}(0.89) M_e^2 \tag{8}$$

yielding:

$$\frac{u}{u_e} = \frac{M}{M_e} \sqrt{\frac{1 + \frac{\gamma - 1}{2} M_e^2}{1 + \frac{\gamma - 1}{2} M^2}} \tag{9}$$

The static pressure was assumed to be constant across the boundary layer, so the density ratio can be written as:

$$\frac{\rho}{\rho_e} = \frac{T_e}{T} = \frac{1 + \frac{\gamma - 1}{2}(0.89)M_e^2}{1 + \frac{\gamma - 1}{2}(0.89)M^2} \tag{10}$$

3.5 BOUNDARY LAYER TEMPERATURE DISTRIBUTION

The temperature distribution across the boundary layer was calculated using the Crocco relation, which is valid for turbulent boundary layers in ideal gases. The Crocco relation is defined as:

$$\frac{T_t}{T_{t_e}} = \frac{T_{t_w}}{T_{t_e}} - \left(\frac{T_{t_w}}{T_{T_e}} - 1\right)\frac{u}{u_e} + 0.2M_e^2\frac{u}{u_e}\left(1 - \frac{u}{u_e}\right) \tag{11}$$

3.6 GENERALIZED VELOCITY

The generalized velocity is the nondimensionalized velocity used for the law-of-the-wall equations. It is defined as such:

$$U^+ = \frac{u^*}{u_\tau} \tag{12}$$

where

$$u^* = \left(u_e/m^{1/2}\right)\sin^{-1}\left(m^{1/2}u/u_e\right) \tag{13}$$

and

$$m = \frac{\left[(\gamma - 1)/2\right]M_e^2}{1 + \left[(\gamma - 1)/2\right]M_e^2} = \frac{0.2M_e^2}{1 + 0.2M_e^2} \tag{14}$$

Remember that:

$$u_\tau = \sqrt{\tau_w/\rho} \tag{15}$$

Chapter IV

Results

The plots in this section are sample plots. For a complete set of plots refer to Grosser (1996).

4.1 VERIFYING A TURBULENT BOUNDARY LAYER

The boundary layers under investigation were verified to be fully turbulent by comparing the measured profiles with the theoretical law-of-the-wall for a fully turbulent boundary layer. The velocity profiles measured with the smallest diameter probe in each facility were transformed to law-of-the-wall coordinates using equations (12) to (15). The friction velocity (u_τ) used to nondimensionalize the law-of-the-wall variables was deduced from Preston tube data obtained in each facility. The calibration procedure for determining the friction velocity is described in appendix B.

An example of measured velocity profiles in law-of-the-wall coordinates is shown in figures 4.1. The theoretical law-of-the-wall profile using typical values for the Von Karman constant (κ) and the intercept constant (C) is shown for comparison. The plots matches well, verifying that the boundary layers in the three NASA facilities are fully turbulent.

4.2 TRUE MACH PROFILE

To calculate the true Mach number, M_o (where here the "o" subscript denotes conditions for D = 0 probe), in each facility the Mach numbers of all data probes were plotted against probe diameter for each Mach number top plot of figure 4.2. A straight line was then fitted through the plotted points and the line was extrapolated to D = 0. The resulting M_o points were plotted against the distance from the wall and compared to each facility's smallest diameter boundary layer survey probe, (right hand plots of figs. 4.2 bottom plot in figure 4.2. For all three test sets, the comparisons were good, so the calculated M_o values were assumed to be the true Mach profiles.

4.3 BOUNDARY LAYER THICKNESS

In order to determine the true boundary layer thickness for each operating condition, the true Mach number profile (M_o) was first converted to a velocity profile (u_o) assuming a temperature distribution based on the Crocco relation (eq. (11)). The true boundary layer thicknesses, δ's, were then defined as the y-positions where $u/u_e = 0.995$.

4.4 CENTERLINE OFFSET

Once the δ's had been calculated, they were used to nondimensionalize the linear distances and all y's were replaced by y/δ. The diameter offset of each probe could now be shown graphically by plotting M/M_e against y/δ, as is done in figure 4.3 (fig. 4.3 is a plot of the 10×10 ft SWT data which exhibited the most extreme offsets). To calculate the actual offset values a horizontal line was drawn from each point to the ideal Mach curve figures 4.4. The magnitude of this horizontal line was Δ/δ, and Δ was calculated simply by multiplying Δ/δ by δ. All of the Δ's were plotted against y/d and an average value was determined by fitting a straight line to the majority of the points, figure 4.5.

In keeping with Allen's methods, the Δ for D = 0 was calculated using a different method. Allen used the slopes of the lines of the top graph in figure 4.2 (∂M/∂D) and the slopes of the true Mach number profiles in the bottom graph of figure 4.2 (∂M/∂y) and the following formulae.

By definition,

$$\frac{M - M_o}{y - y_o} \Rightarrow \frac{\partial M}{\partial y}, \text{as } D \Rightarrow 0 \tag{16}$$

but,

$$y - y_o = \Delta \tag{17}$$

Now, referring to figure 4.2

$$\text{SLOPE} = \frac{\partial M}{\partial D} = \frac{M - M_o}{D - D_o} \tag{18}$$

but $D_o = 0$, so:

$$\frac{\partial M}{\partial D} = \frac{M - M_o}{D} \Rightarrow M - M_o = \frac{\partial M}{\partial D} D \tag{19}$$

plugging equations (17) and (19) into (16) leads to:

$$\frac{\frac{\partial M}{\partial D} D}{\Delta} = \frac{\partial M}{\partial y} \quad \text{or} \quad \frac{\Delta}{D} = \frac{\partial M / \partial D}{\partial M / \partial y} \tag{20}$$

at D = 0. Figure 4.6 show the results of these calculations. The points were averaged to get the Δ/D value for D = 0.

A graph plotting the present study against previous studies is shown in figure 4.7. Figures 4.8 to 4.12 show the centerline offset error, Δ/D, versus D/δ, M_∞, R_∞, ∂M/∂y, and δ. Appendix A contains the resulting M/M_e values for each y/δ for the three NASA facilities. The values for D = 0 are also included for comparison.

4.5 STATISTICAL ANALYSIS

The resulting Δ/D values and their corresponding Mach numbers, Reynolds numbers, and D/δ values were entered into RS1, a statistical analysis program by BBN Software Products, to determine which properties significantly influenced Δ/D. Table IV lists the model terms entered into RS1.

All properties in table IV were first normalized by RS1 so that they ranged between ±1. RS1 then created more terms through combinations and second order terms. From the analysis RS1 gave a significance for each factor, indicating which factors were <u>not</u> important and, thus, which factors should be removed for the next analysis. The analysis was originally run without the 15×15 cm SWT, $R_\infty = 6.00 \times 10^6$/m dataset (this dataset was run later) and the results yielded a strong freestream Reynolds number dependence and a slight freestream Mach number dependence. RS1 generated the coefficients for a second order function, and the resulting function was:

$$\frac{\Delta}{D} = 0.582205 + 0.057790\left(M'_\infty\right) + 0.928536\left(R'_\infty\right) + 0.099388\left(M'_\infty\right)\left(R'_\infty\right) + 0.178375\, R'^{\,2}_\infty \tag{21}$$

where M'_∞ and R'_∞ are the normalized freestream Mach number and normalized freestream Reynolds number and are defined as:

$$R'_\infty = \frac{1/R_\infty - 1.466818 \times 10^{-7}}{8.751022 \times 10^{-8}} \tag{22}$$

$$M'_\infty = \frac{M_\infty - 2.26}{0.3} \tag{23}$$

Additional data were then taken in the 15×15 cm SWT tunnel at a new Reynolds number (6.00×10^6/m) to see if its offset values conformed to the values predicted by equation (21). The new offset values did <u>not</u> equal the values predicted by equation (21), so the statistical analysis was run again, this time with the new 15×15 cm SWT data included. Instead of freestream Reynolds number, Reynolds number based on probe diameter, R_D, was used (actually, R_∞ was first used, then switched to R_D). RS1 indicated that R_D, D/δ, and δ were not significant factors in the pitot probe centerline displacement. It indicated that with the data given, the significant factors were Mach gradient, $\partial M/\partial y$, and freestream Mach number, M_∞. The calculated coefficients yielded the following equation:

$$\frac{\Delta}{D} = 1.453183 + 0.187443\left(M'_\infty\right) + 0.998\left(\frac{\partial M'}{\partial y}\right) - 0.748158\left(\frac{\partial M'}{\partial y}\right)^2 \tag{24}$$

where R'_∞ and M'_∞ are defined in equations (22) and (23) and $\partial M'/\partial y$ is defined as:

$$\left(\partial M'/\partial y\right) = \frac{\left(1/\left(\partial M/\partial y\right)\right) - 1.3094945}{0.01195055} \tag{25}$$

same as before. Figure 4.13 shows a three-dimensional plot of these results.

Chapter V

Conclusion

The purpose of this research was to create a supersonic, turbulent boundary layer dataset and to attempt to define the factors influencing pitot probe centerline displacement error in such a flowfield. An additional purpose was to formulate the relationship between the offset error and its factors. This research has indeed created a dataset for this flowfield, but it has also indicated the need for more data. The data taken proved to be a small part in a very large and complex picture. Nonetheless, the statistical analysis program RS1 was used to fit the existing data and generated the following formula:

$$\frac{\Delta}{D} = 1.453183 + 0.187443\left(M'_{\infty}\right) + 0.998\left(\frac{\partial M'}{\partial y}\right) - 0.748158\left(\frac{\partial M'}{\partial y}\right)^2$$

where the primed values are defined in equations (22) and (25).

Figures 4.08 to 4.12 plot all the factors separately and figure 4.13 gives a three-dimensional graph of this formula. Referring to figure 4.11 it looks as if the error relation increases asymptotically as $\partial M/\partial y$ goes to zero, but logically, that is not true. In reality, a point must exist at 0.0, 0.0 indicating that in the freestream the probes read the correct pressures (which they did in all experiments). This generates some interesting questions about what is happening to the correction curve between $\partial M/\partial y$ = 0.000/mm and $\partial M/\partial y$ = 0.030/mm. Unfortunately, the statistical analysis program RS1 could not generate an accurate function with the 0.0, 0.0 point without more data. Figure 5.1 illustrates the possible curves RS1 might generate without additional data to fill the 0.000/mm < $\partial M/\partial y$ < 0.030/mm gap. Answers can only be found with more experimentation.

Another noteworthy point is that as Mach number decreases, and, specifically, when M<1.0, Δ/D becomes less than one. This is very important because it indicates that the shock in the supersonic boundary layer is skewing the flow and causing the probe to read a pressure outside the diameter of the probe (something that did not seem physically possible). Again, more data is needed to define exact limits.

The results from this research can be summarized as thus:

1. In a supersonic turbulent boundary layer the pitot probe centerline offset error, Δ/D, is not greatly influenced by the probe diameter, D/δ, the boundary layer thickness, δ, or the Reynold numbers R_{∞} or $R_{D.}$
2. The pitot probe centerline displacement error is influenced by the Mach gradient, $\partial M/\partial y$, and the freestream Mach number, M_{∞}.
3. $\Delta/D = 1.453183 + 0.187443\ (M'_{\infty}) + 0.998(\partial M'/\partial y) - 0.748158(\partial M'/\partial y)^2$ appears to describe the relationship between offset error and test conditions for 0.030/mm <$\partial M/\partial y$ <0.100/mm. Primed variables are defined in equations (22) and (25). This equation must go to zero as $\partial M/\partial y$ goes to zero.
4. More data is needed to complete the supersonic, turbulent boundary layer matrix and to allow for more accurate formulation.

5. Future work should include a repeat of the 10×10 ft SWT $M_\infty = 2.00$ and $M_\infty = 2.56$ data and should also attempt to fill the gaps between 0.000/mm $< \partial M/\partial y <$ 0.030/mm. This may be achieved by running the 10×10 ft SWT at higher Mach numbers.

6. It appears that for most supersonic, turbulent boundary layer research the correction factor lies near zero. Thus, for research in tunnels where $\partial M/\partial y$ is greater than 0.030/mm, a correction factor is not needed.

BIBLIOGRAPHY

Allen, Jerry M.: Pitot-Probe Displacement in a Supersonic Turbulent Boundary Layer, NASA TN D–6759, April 1972.

Allen, Jerry M.: Evaluation of Compressible-Flow Preston Tube Calibrations, NASA TN D–7190, 1973.

Allen, Jerry M.: Reevaluation of Compressible-Flow Preston Tube Calibrations, NASA TM X–3488, 1977.

Bradshaw, P.; and Unsworth, K.: A Note on Preston Tube Calibrations in Compressible Flow. IC Aero. Rep. 73–07, Dep. Aeronaut., Imperial College Sci. & Technol., Sept. 1973.

Bryer, D.W.; and Pankhurst, R.C.: Pressure-probe Methods for Determining Wind Speed and Flow Direction, 1971.

Chue, S.H.: Pressure Probes for Fluid Measurement, Prog. Aerospace Sci., 1975, Vol. 16, No. 2, pp. 147–223.

Davies, F.V.: Some Effects of Pitot Size on the Measurement of Boundary Layers in Supersonic Flow, Tech. Note No. Aero. 2179, Brit. R.A.E., August, 1952.

Davies, P.O.A.L.: The Behavior of a Pitot Tube in Transverse Shear, J. Fluid Mech., Vol. 3, pt. 5, February 1958, pp. 441–456.

Fenter, Felix W.; and Stalmach, Charles, J., Jr.: The Measurement of Local Turbulent Skin Friction at Supersonic Speeds by Means of Surface Impact Pressure Probes. DRL-32, CM-878 (Contract Nord-16498), Univ. of Texas, Oct. 21, 1957.

Grosser, Wendy I.; Factors Influencing Pitot Probe Centerline Displacement in a Supersonic Turbulent Boundary Layer, Cleveland State University, 1996.

Hopkins, Edward J.; and Keener, Earl R.: Study of Surface Pitots for Measuring Turbulent Skin Friction at Supersonic Mach Numbers—Adiabatic Wall. NASA TN D–3478, 1966

Livesey, J.L.: Behavior of Transverse Cylindrical and Forward Facing Total Pressure Probes in Transverse Total Pressure Gradients, J. Aeronaut Sci., Vol. 23, No. 10, October 1956, pp. 949–955.

MacMillan, F.A.: Experiments on Pitot-Tubes in Shear Flow, R. & M. No. 3028, Brit. A.R.C., 1957.

Peterson, John B., Jr.: Boundary-Layer Velocity Profiles Downstream of Three-Dimensional Transition Trips on a Flat Plate at Mach 3 and 4, NASA TN D–5523, 1969.

Sigalla, Armand: Calibration of Preston Tubes in Supersonic Flow. AIAA J., Vol. 3, No. 8, Aug. 1965, p. 1531.

Young, A.D. and Maas, J.N.: The Behaviour of a Pitot Tube in a Transverse Total Pressure Gradient, R&M. No. 1770, Brit. A.R.C., 1937.

APPENDIX A

SUMMARY OF REDUCED DATA

Summary of Reduced 10×10 ft SWT Data; $M_\infty = 2.00$, $R_\infty = 4.27 \times 10^6$/m

	M/Me				
y/delta	**D=12.7 cm**	**D=9.525 cm**	**D=6.35 cm**	**D=3.175 cm**	**D=0 cm**
0.06	0.672	0.667	0.652	0.633	0.623
0.11	0.731	0.717	0.706	0.690	0.678
0.17	0.762	0.751	0.742	0.726	0.716
0.22	0.789	0.779	0.770	0.755	0.745
0.28	0.815	0.803	0.795	0.781	0.771
0.34	0.839	0.826	0.821	0.804	0.795
0.39	0.862	0.848	0.841	0.827	0.816
0.45	0.881	0.868	0.862	0.848	0.838
0.51	0.900	0.889	0.883	0.868	0.860
0.56	0.918	0.905	0.901	0.887	0.879
0.62	0.933	0.924	0.917	0.906	0.897
0.67	0.949	0.940	0.934	0.924	0.917
0.73	0.961	0.953	0.949	0.940	0.934
0.79	0.972	0.966	0.961	0.955	0.950
0.84	0.981	0.977	0.974	0.967	0.963
0.90	0.989	0.986	0.984	0.980	0.977
0.96	0.993	0.991	0.990	0.988	0.986
1.00	0.996	0.995	0.995	0.992	0.991
1.01	0.997	0.996	0.996	0.993	0.993
1.07	0.999	0.998	1.000	0.997	0.997
1.12	1.000	1.000	1.001	0.999	0.999
1.18	1.001	1.001	1.002	1.001	1.002
1.24	1.002	1.002	1.002	1.002	1.003
1.29	1.002	1.003	1.003	1.003	1.004
1.35	1.003	1.003	1.003	1.003	1.003
1.41	1.003	1.003	1.003	1.003	1.003

Summary of Reduced 10×10 ft SWT Data; $M_\infty = 2.56$, $R_\infty = 4.27 \times 10^6$/m

	M/Me				
y/delta	**D=12.7 cm**	**D=9.525 cm**	**D=6.35 cm**	**D=3.175 cm**	**D=0 cm**
0.04	0.609	0.585	0.574	0.543	0.526
0.08	0.666	0.642	0.629	0.607	0.589
0.12	0.693	0.674	0.664	0.645	0.630
0.17	0.719	0.701	0.690	0.674	0.660
0.21	0.744	0.724	0.715	0.699	0.685
0.25	0.766	0.746	0.737	0.721	0.706
0.29	0.787	0.767	0.756	0.743	0.727
0.33	0.807	0.787	0.776	0.761	0.746
0.37	0.828	0.807	0.797	0.781	0.765
0.41	0.847	0.825	0.816	0.802	0.786
0.46	0.865	0.843	0.833	0.821	0.805
0.50	0.883	0.861	0.851	0.839	0.823
0.54	0.898	0.878	0.868	0.857	0.841
0.58	0.914	0.894	0.885	0.873	0.859
0.62	0.929	0.909	0.901	0.890	0.876
0.66	0.945	0.924	0.917	0.906	0.892
0.70	0.958	0.939	0.932	0.922	0.909
0.74	0.967	0.952	0.944	0.937	0.925
0.79	0.977	0.963	0.957	0.950	0.940
0.83	0.984	0.974	0.967	0.962	0.954
0.87	0.989	0.982	0.975	0.971	0.964
0.91	0.993	0.987	0.984	0.981	0.976
0.95	0.996	0.992	0.990	0.987	0.984
0.99	0.998	0.995	0.993	0.991	0.988
1.00	0.998	0.996	0.993	0.991	0.989
1.03	0.999	0.998	0.996	0.995	0.993

Summary of Reduced 1 × 1 ft SWT Data; $M_\infty = 1.96$, $R_\infty = 16.9 \times 10^6$/m

	M/Me				
y/delta	**D=0.210 cm**	**D=0.147 cm**	**D=0.090 cm**	**D=0.051 cm**	**D=0 cm**
0.09	0.635	0.628	0.622	0.634	0.627
0.14	0.676	0.667	0.662	0.671	0.663
0.19	0.705	0.698	0.695	0.703	0.697
0.24	0.726	0.724	0.720	0.730	0.726
0.29	0.748	0.747	0.745	0.754	0.752
0.34	0.774	0.770	0.768	0.777	0.773
0.39	0.796	0.794	0.792	0.798	0.796
0.44	0.816	0.815	0.813	0.820	0.818
0.49	0.836	0.835	0.832	0.840	0.838
0.54	0.855	0.855	0.854	0.861	0.860
0.59	0.876	0.875	0.873	0.880	0.878
0.64	0.897	0.896	0.896	0.900	0.899
0.69	0.914	0.913	0.915	0.919	0.918
0.74	0.929	0.929	0.933	0.936	0.937
0.79	0.944	0.947	0.946	0.950	0.951
0.84	0.957	0.957	0.962	0.963	0.966
0.89	0.970	0.969	0.971	0.975	0.975
0.94	0.980	0.978	0.983	0.985	0.985
0.99	0.986	0.987	0.987	0.991	0.991
1.00	0.987	0.988	0.988	0.991	0.992
1.04	0.990	0.991	0.990	0.995	0.994
1.09	0.991	0.991	0.991	0.997	0.996
1.14	0.991	0.995	0.994	0.998	0.999
1.19	0.994	0.995	0.994	0.998	0.998
1.24	0.995	0.995	0.994	0.999	0.998
1.29	0.995	0.995	0.994	1.000	0.999

Summary of Reduced 1 × 1 ft SWT Data; $M_\infty = 2.46$, $R_\infty = 16.9 \times 10^6$/m

	M/Me				
y/delta	**D=0.210 cm**	**D=0.147 cm**	**D=0.090 cm**	**D=0.051 cm**	**D=0 cm**
0.09	0.594	0.588	0.588	0.588	0.585
0.14	0.634	0.632	0.632	0.632	0.630
0.19	0.663	0.665	0.665	0.665	0.667
0.25	0.688	0.692	0.692	0.692	0.694
0.30	0.711	0.716	0.716	0.716	0.718
0.35	0.736	0.739	0.739	0.739	0.741
0.40	0.762	0.763	0.763	0.763	0.763
0.45	0.785	0.785	0.785	0.785	0.786
0.50	0.808	0.809	0.809	0.809	0.810
0.56	0.830	0.831	0.831	0.831	0.832
0.61	0.852	0.855	0.855	0.855	0.856
0.66	0.873	0.877	0.877	0.877	0.878
0.71	0.895	0.900	0.900	0.900	0.903
0.76	0.915	0.919	0.919	0.919	0.921
0.81	0.933	0.938	0.938	0.938	0.940
0.87	0.950	0.955	0.955	0.955	0.957
0.92	0.966	0.968	0.968	0.968	0.970
0.97	0.978	0.982	0.982	0.982	0.983
1.00	0.984	0.988	0.988	0.988	0.990
1.02	0.987	0.992	0.992	0.992	0.994
1.07	0.993	0.996	0.996	0.996	0.997
1.12	0.996	0.999	0.999	0.999	1.000
1.18	0.998	1.001	1.001	1.001	1.002
1.23	0.999	1.003	1.003	1.003	1.005
1.28	0.998	1.003	1.003	1.003	1.005
1.33	0.998	1.003	1.003	1.003	1.005

Summary of Reduced 1 × 1 ft SWT Data; $M_\infty = 1.96$, $R_\infty = 10.3\times10^6$/m

	M/Me				
y/delta	**D=0.210 cm**	**D=0.147 cm**	**D=0.090 cm**	**D=0.051 cm**	**D=0 cm**
0.08	0.614	0.613	0.609	0.610	0.607
0.12	0.658	0.652	0.649	0.650	0.646
0.17	0.687	0.685	0.681	0.683	0.679
0.21	0.711	0.710	0.711	0.710	0.709
0.26	0.738	0.735	0.733	0.734	0.731
0.30	0.758	0.757	0.756	0.757	0.756
0.35	0.782	0.780	0.778	0.778	0.777
0.39	0.803	0.802	0.800	0.800	0.799
0.44	0.825	0.823	0.820	0.821	0.819
0.48	0.844	0.844	0.842	0.842	0.841
0.53	0.864	0.864	0.863	0.863	0.862
0.57	0.885	0.884	0.884	0.883	0.883
0.62	0.903	0.901	0.903	0.902	0.902
0.66	0.920	0.921	0.921	0.919	0.919
0.71	0.937	0.938	0.938	0.936	0.937
0.75	0.953	0.952	0.953	0.952	0.952
0.80	0.966	0.965	0.966	0.965	0.965
0.84	0.976	0.975	0.976	0.975	0.975
0.89	0.984	0.984	0.983	0.982	0.983
0.93	0.989	0.989	0.989	0.988	0.988
0.98	0.992	0.992	0.992	0.991	0.991
1.00	0.993	0.993	0.993	0.992	0.992
1.02	0.994	0.993	0.993	0.993	0.992
1.07	0.995	0.995	0.995	0.994	0.994
1.11	0.996	0.995	0.995	0.995	0.995
1.16	0.997	0.996	0.996	0.996	0.995

Summary of Reduced 1 × 1 ft SWT Data; $M_\infty = 2.46$, $R_\infty = 10.3\times10^6$/m

	M/Me				
y/delta	**D=0.210 cm**	**D=0.147 cm**	**D=0.090 cm**	**D=0.051 cm**	**D=0 cm**
0.08	0.571	0.567	0.563	0.569	0.565
0.13	0.616	0.607	0.605	0.612	0.606
0.18	0.647	0.641	0.640	0.645	0.641
0.23	0.672	0.669	0.666	0.673	0.669
0.28	0.696	0.693	0.690	0.697	0.693
0.32	0.721	0.719	0.714	0.721	0.717
0.37	0.746	0.743	0.738	0.745	0.741
0.42	0.768	0.767	0.763	0.769	0.766
0.47	0.793	0.790	0.787	0.792	0.789
0.52	0.815	0.814	0.810	0.815	0.812
0.56	0.836	0.835	0.834	0.837	0.836
0.61	0.859	0.857	0.855	0.859	0.857
0.66	0.880	0.879	0.877	0.880	0.878
0.71	0.900	0.899	0.899	0.900	0.899
0.76	0.921	0.918	0.918	0.920	0.918
0.80	0.939	0.937	0.937	0.938	0.937
0.85	0.954	0.953	0.953	0.955	0.955
0.90	0.969	0.968	0.969	0.970	0.970
0.95	0.981	0.979	0.980	0.981	0.981
1.00	0.989	0.988	0.989	0.989	0.989
1.00	0.989	0.988	0.989	0.990	0.990
1.04	0.994	0.993	0.994	0.995	0.995
1.09	0.996	0.996	0.997	0.997	0.998
1.14	0.998	0.998	0.998	0.999	0.999
1.19	0.998	0.998	0.999	0.999	1.000
1.24	0.998	0.998	0.999	0.999	1.000

Summary of Reduced 15 × 15 cm SWT Data; $M_\infty = 2.47$, $R_\infty = 10.3 \times 10^6$/m

	M/Me				
y/delta	D=0.210 cm	D=0.147 cm	D=0.090 cm	D=0.051 cm	D=0 cm
0.12	0.592	0.589	0.591	0.593	0.592
0.17	0.638	0.624	0.625	0.627	0.620
0.21	0.669	0.655	0.654	0.655	0.648
0.26	0.689	0.679	0.679	0.680	0.675
0.30	0.714	0.699	0.703	0.706	0.700
0.35	0.732	0.720	0.727	0.729	0.726
0.39	0.753	0.749	0.752	0.750	0.749
0.44	0.779	0.770	0.776	0.772	0.770
0.48	0.802	0.790	0.796	0.791	0.788
0.53	0.823	0.810	0.816	0.812	0.809
0.58	0.842	0.836	0.835	0.835	0.832
0.62	0.861	0.859	0.859	0.855	0.854
0.67	0.882	0.869	0.880	0.876	0.875
0.71	0.904	0.897	0.896	0.898	0.894
0.76	0.921	0.920	0.918	0.914	0.913
0.80	0.938	0.934	0.938	0.933	0.933
0.85	0.953	0.944	0.952	0.949	0.949
0.89	0.963	0.960	0.970	0.962	0.966
0.94	0.973	0.975	0.980	0.974	0.977
0.98	0.986	0.983	0.990	0.984	0.987
1.00	0.991	0.986	0.994	0.988	0.990
1.03	0.998	0.990	0.999	0.994	0.994
1.07	0.999	0.997	1.002	0.998	0.999
1.12	1.002	0.999	1.002	1.002	1.002
1.16	1.002	1.002	1.002	1.001	1.001
1.21	1.002	1.001	1.001	1.001	1.001

Summary of Reduced 15 × 15 cm SWT Data; $M_\infty = 2.47$, $R_\infty = 6.00 \times 10^6$/m

	M/Me				
y/delta	D=0.210 cm	D=0.147 cm	D=0.090 cm	D=0.051 cm	D=0 cm
0.12	0.567	0.569	0.569	0.578	0.578
0.16	0.609	0.602	0.604	0.610	0.607
0.20	0.639	0.634	0.629	0.635	0.630
0.24	0.669	0.657	0.654	0.661	0.653
0.28	0.688	0.681	0.677	0.685	0.679
0.32	0.711	0.703	0.701	0.706	0.701
0.36	0.728	0.722	0.723	0.727	0.724
0.41	0.750	0.746	0.744	0.751	0.747
0.45	0.774	0.765	0.764	0.771	0.765
0.49	0.795	0.788	0.785	0.792	0.787
0.53	0.814	0.807	0.806	0.810	0.806
0.57	0.833	0.830	0.827	0.831	0.828
0.61	0.852	0.845	0.847	0.853	0.850
0.65	0.871	0.870	0.867	0.871	0.868
0.69	0.889	0.887	0.883	0.889	0.886
0.73	0.910	0.905	0.901	0.907	0.902
0.78	0.929	0.921	0.920	0.922	0.918
0.82	0.942	0.938	0.937	0.940	0.937
0.86	0.958	0.952	0.950	0.955	0.950
0.90	0.969	0.965	0.967	0.968	0.967
0.94	0.981	0.977	0.980	0.978	0.978
0.98	0.991	0.987	0.988	0.987	0.985
1.00	0.994	0.991	0.991	0.991	0.990
1.02	0.997	0.995	0.996	0.995	0.994
1.06	1.003	1.001	1.001	1.002	1.000
1.10	1.006	1.005	1.005	1.005	1.005

APPENDIX B

CALCULATION OF C_f

CALCULATION OF C_f

C_f is defined as $(2\tau_w)/(\rho u)$ and was calculated by using the Bradshaw-Unsworth (1974), equation. This equation was chosen over Sigalla (1965) and Fenter-Stalmach (1957) because it is based on the law-of-the-wall equations and not on the power-law equations. Bradshaw and Unsworth used a Preston tube—a circular pitot tube resting on the surface—to measure the total pressure at the wall. This pressure is then plugged into an equation and the equation is solved for C_f. The Bradshaw-Unsworth equation is as follows:

$$P_\tau = 96 + 60\log_{10}\left(\frac{R_\tau}{50}\right) + 2.37\left[\log_{10}\left(\frac{R_\tau}{50}\right)\right]^2 + 10^4 M_\tau^2\left(R_\tau^{0.30} - 2.38\right)$$

where

$$P_\tau = \frac{P_{t_{wall}} - p_s}{\tau_{wall}}$$

$$R_\tau = \frac{D}{\mu_w}\sqrt{\tau_t \rho_w}$$

$$M_\tau = \frac{\sqrt{\tau_t}}{a_w\sqrt{\rho_w}}$$

TABLE I.—SUMMARY OF PREVIOUS RESEARCH

Investigator	D/δ	Mach Number	Reynolds Number per meter	Flow Conditions	General Results
Young & Maas	0.02 to 0.27	Incompressible	1.3×10^6	Wake	Δ/D=0.18
F. Davies	0.18 to 1.18	2.3	10.0×10^6 to 12.0×10^6	Laminar B.L. (flat plate & cone)	No displacement
Livesey	0.01 to 0.13	Incompressible	0.5×10^6	Turbulent B.L.	Δ/D=0.09
P. Davies	0.04 to 0.69	Incompressible	1.5×10^6	Turbulent B.L. Wake	No displacement
MacMillan	0.02 to 0.12	Incompressible	0.5 to 2.3×10^6	Turbulent B.L. Turbulent Pipe	Δ/D=0.15 for y/d>2
Allen	0.018 to 0.691	2.0	8×10^6	Turbulent B.L.	Δ/D=0.38 for D=0

TABLE II.—SUMMARY OF RESEARCH VARIABLES

Facility	**Nom. Mach**	**Freestream Reynolds Number**	**Approx. Boundary Layer Thickness**	**D/δ**			
10 ft x 10 ft SWT	2.00 2.56	4.27×10^6/m	224 mm 205 mm	.015	.030	.045	.060
15 cm x 15 cm SWT	2.47	10.3×10^6/m 6.00×10^6/m	12.7 mm 13.0 mm	.039	.072	.121	.167
1 ft x 1 ft SWT	1.96 2.46 1.96 2.46	10.3×10^6/m 16.9×10^6/m	29.3 mm 27.5 mm 26.4 mm 25.5 mm	.016	.030	.053	.070
4 ft x 4 ft** SWT (Allen)	2.0	8.0×10^6/m	69.9 mm	.018	.034	.145	.256

** Allen also ran D/δ = .364, .473, .582, .691.

TABLE III.—TUNNEL FREESTREAM CONDITIONS

Facility	M	Re_∞ (/m)	P_t (ka)	T_t (°C)
10 ft x 10 ft* SWT	2.00 2.56	4.26×10^6	33.8 44.8	27
15 cm x 15 cm SWT	2.47	10.3×10^6 6.00×10^6	103.4 61.2	27 24
1 ft x 1 ft SWT	1.96 2.46	10.3×10^6 16.9×10^6	131.0	19
4 ft x 4 ft SWT (Allen)	2.00	8.0×10^6	202.6	43

* For the 0.051 cm diameter probe at M=2.56, P_t = 56.2 ka and T_t = 37 °C.

TABLE IV.—LIST OF RS1 MODEL TERMS

Item	Model Term
1	D/δ
2	M_∞
3	R_∞
4	$\partial M/\partial y$
5	δ

TABLE V.—LIST OF Δ/D, M_∞,R_∞, AND D/δ VALUES

	Δ/D	D/δ	Mach Number	Reynolds Number per meter	$\partial M/\partial y$ per mm	δ mm
10 ft x 10 ft Data	0.962	0.000	2.00	4.27E+06	0.004	224.0
	1.321	0.014				
	1.693	0.029				
	1.484	0.042				
	1.594	0.057				
	1.661	0.000	2.56	4.27E+06	0.006	205.0
	1.984	0.016				
	1.721	0.031				
	1.864	0.046				
	2.083	0.062				
1 ft x 1 ft Data	0.088	0.000	1.96	10.3E+06	0.029	29.3
	0.033	0.017				
	0.090	0.031				
	0.064	0.050				
	0.072	0.072				
	0.029	0.000	2.46	10.3E+06	0.041	27.5
	0.220	0.019				
	-0.122	0.033				
	-0.012	0.053				
	0.049	0.076				
1 ft x 1 ft Data	-0.123	0.000	1.96	16.9E+06	0.028	26.4
	0.108	0.019				
	-0.369	0.034				
	-0.228	0.057				
	-0.140	0.080				
	-0.096	0.000	2.46	16.9E+06	0.040	25.5
	-0.205	0.020				
	-0.114	0.036				
	-0.071	0.058				
	-0.114	0.083				
15 cm x 15 cm Data	0.062	0.000	2.47	10.3E+06	0.088	12.7
	0.101	0.166				
	-0.006	0.116				
	0.130	0.072				
	0.083	0.040				
15 cm x 15 cm Data	0.043	0.000	2.47	6.00E+06	0.091	13.0
	0.085	0.166				
	0.010	0.116				
	-0.021	0.072				
	0.203	0.040				
4 ft x 4 ft Data (Allen's Data)	0.480	0.000	2.00	8.00E+06	0.020	69.9
	0.500	0.010				
	0.520	0.034				

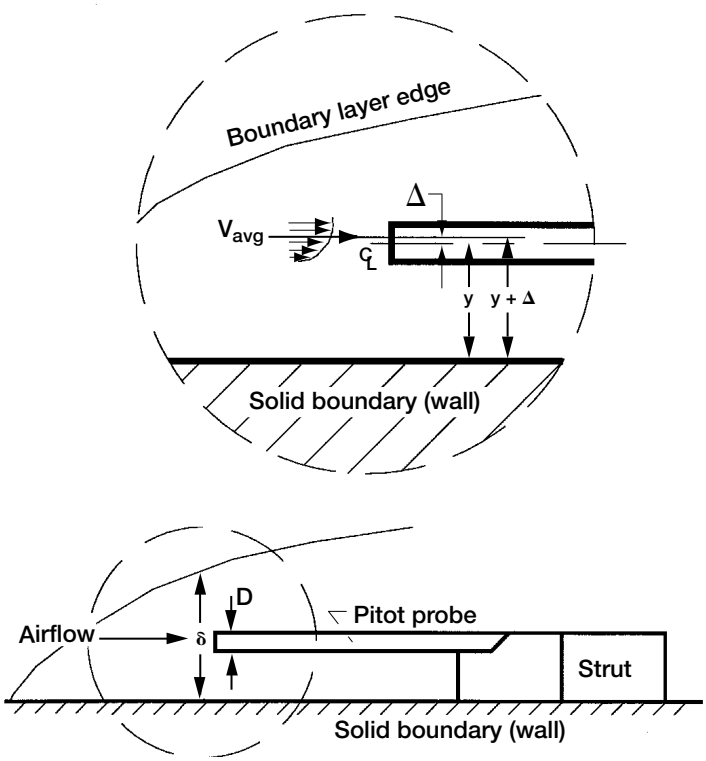

Figure 1.1.—Illustration of centerline displacement effect.

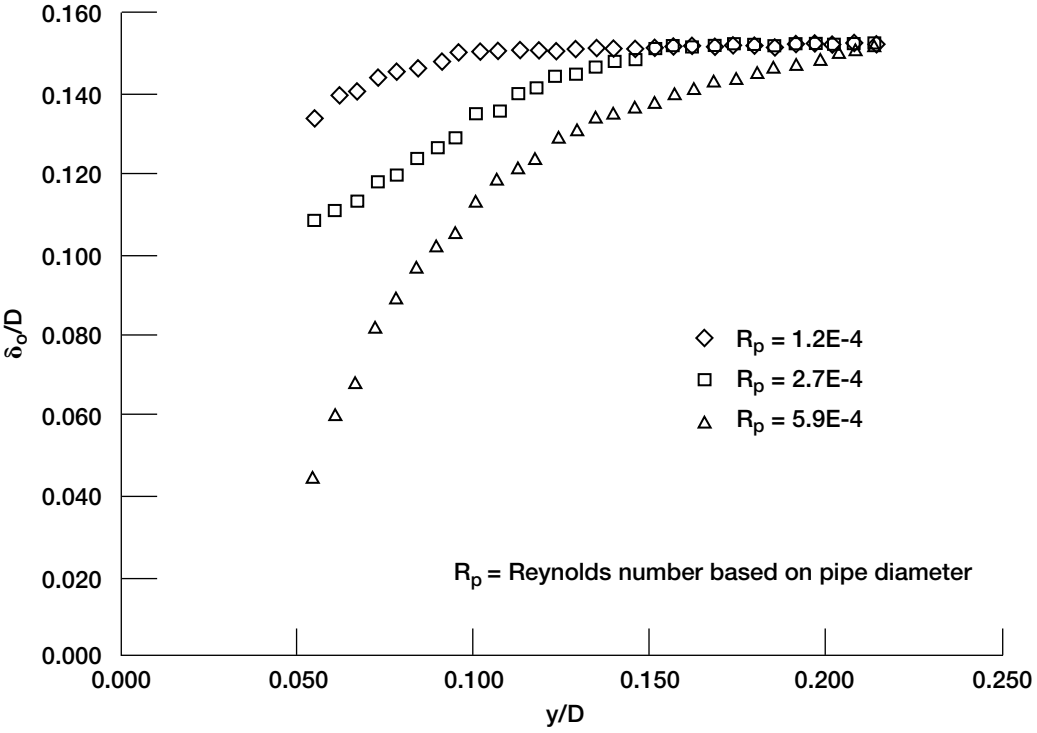

Figure 1.2.—MacMillan's apparent displacement δ_o.

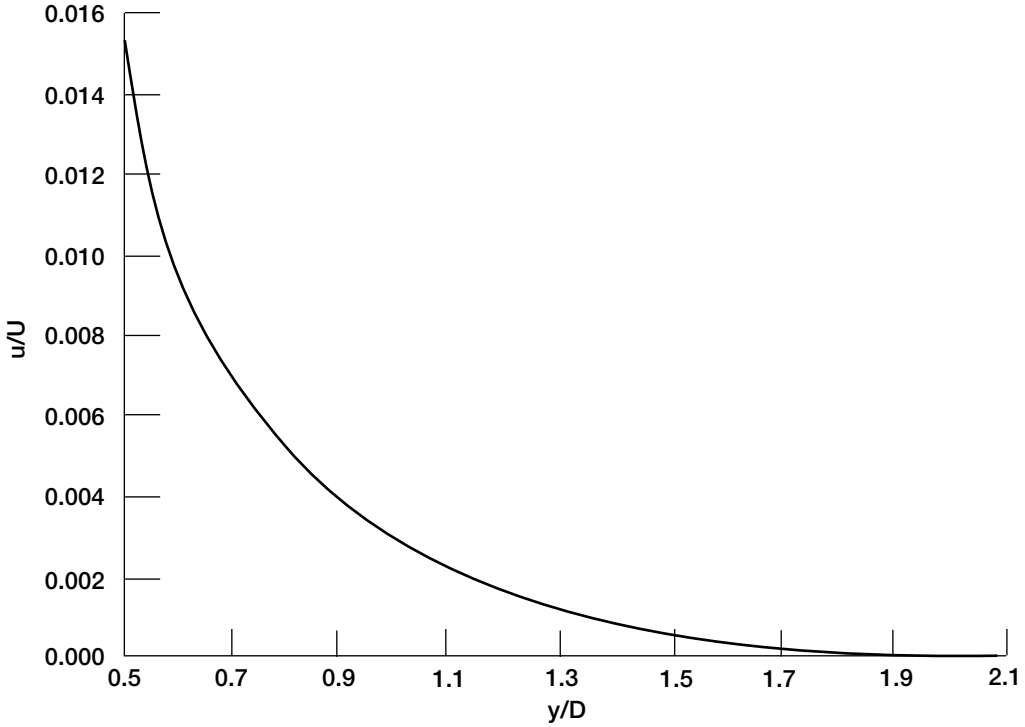

Figure 1.3.—MacMillan's wall effect expressed as a function of y/D.

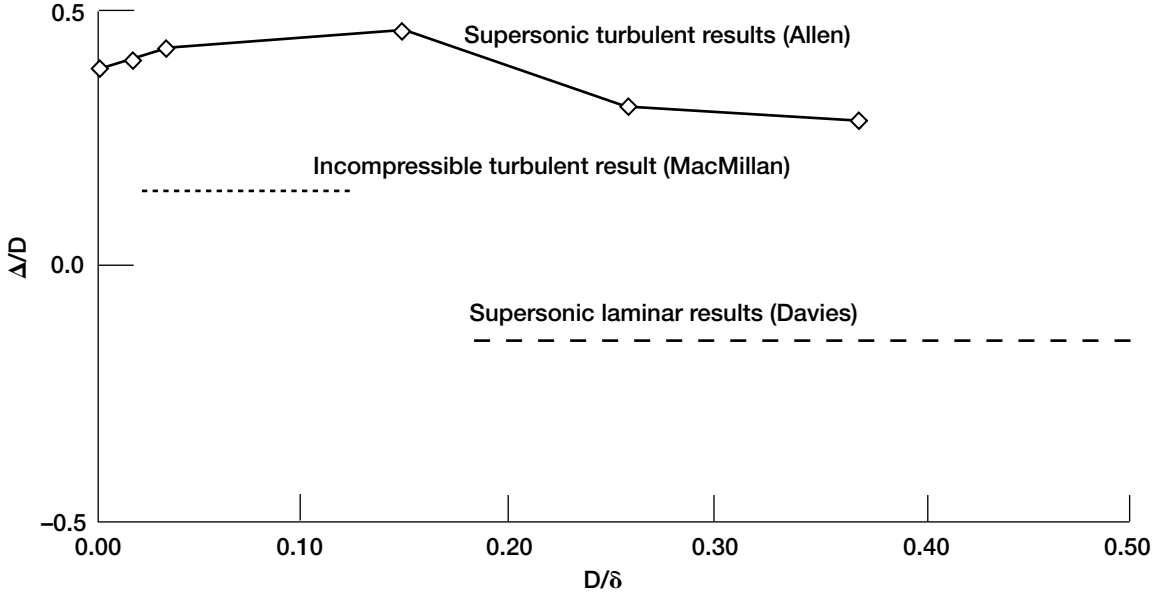

Figure 1.4.—Summary of previous results on centerline displacement error.

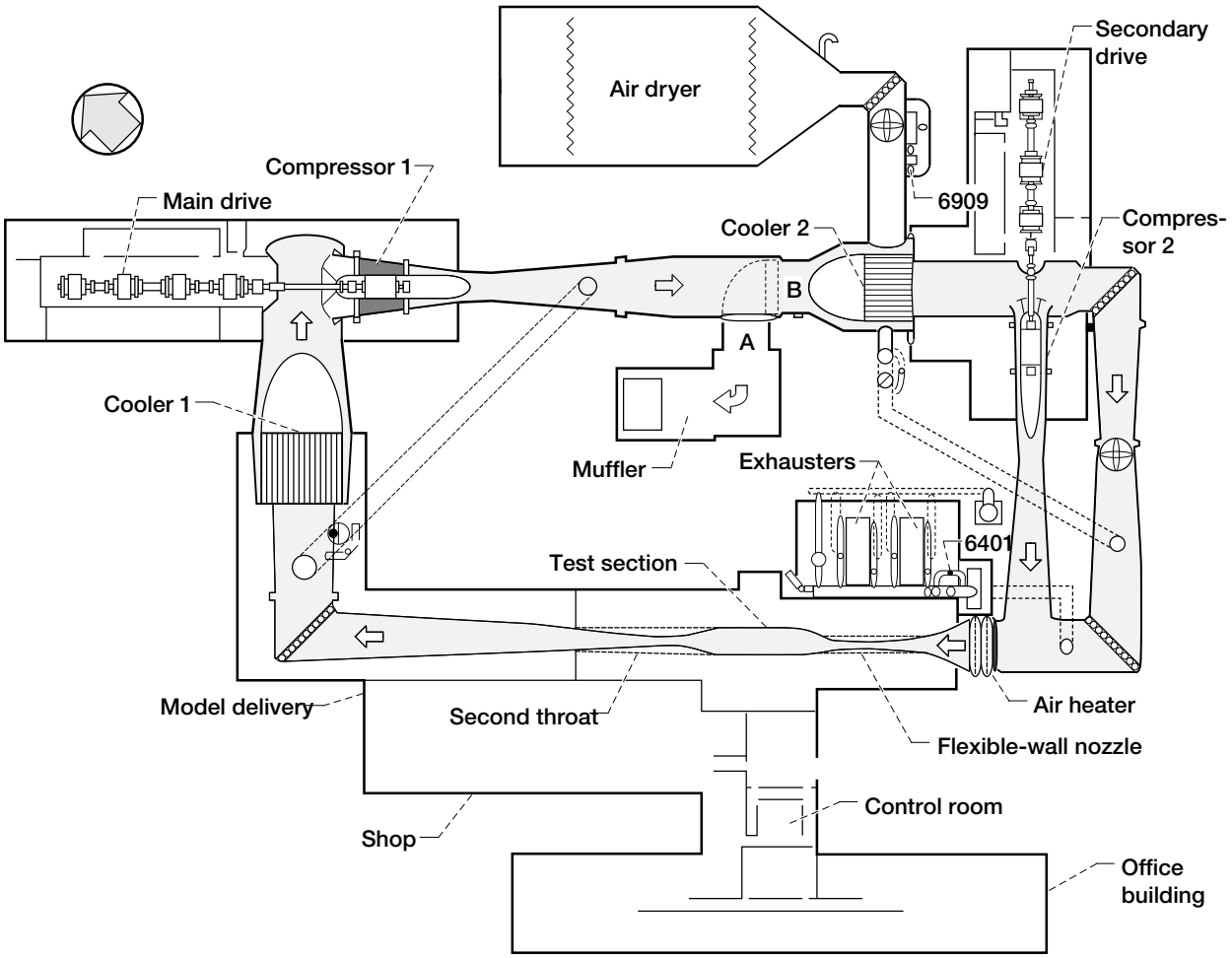

Figure 2.1.—Plan form view of the NASA Lewis 10 ft x 10 ft Supersonic Wind Tunnel.

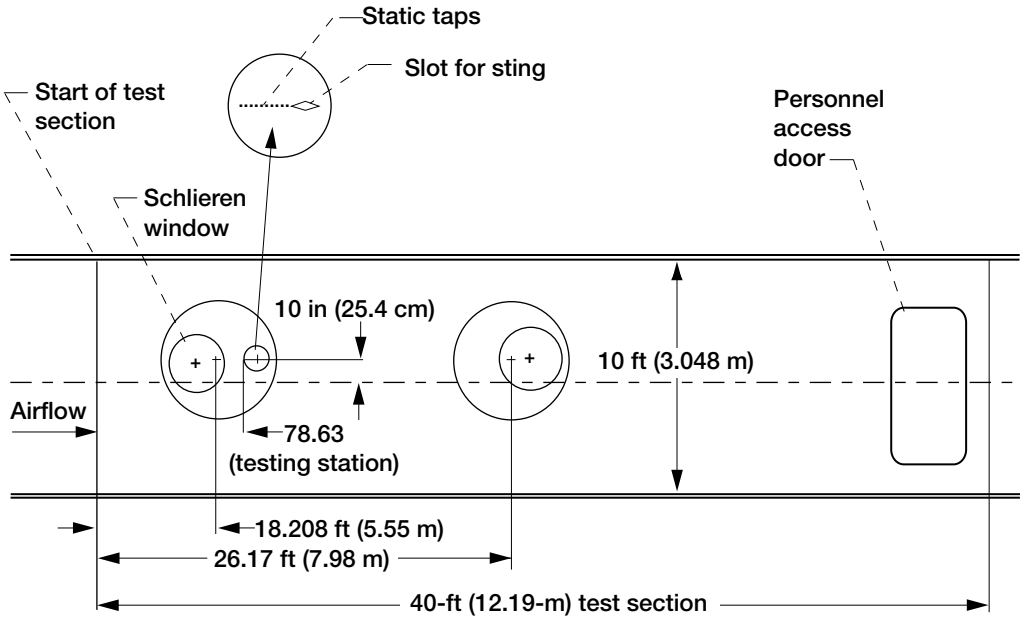

Figure 2.2.—Elevation view of the 10 ft x 10 ft SWT Test section.

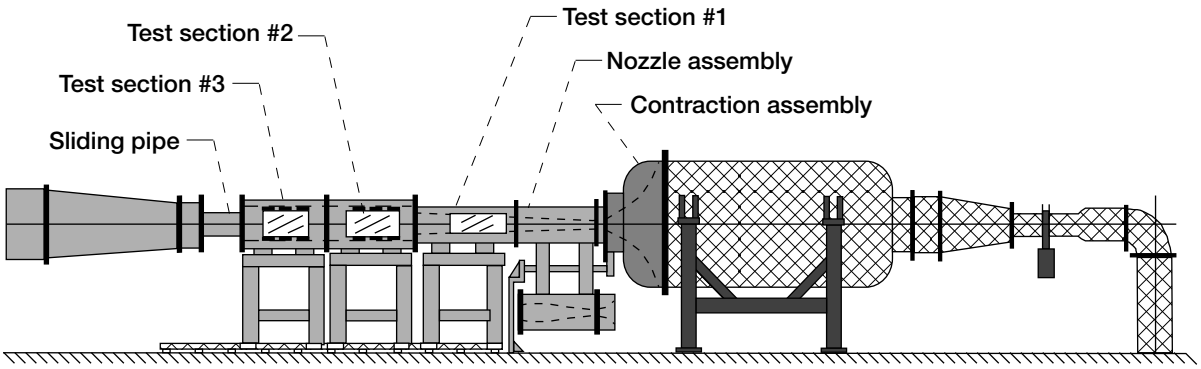

Figure 2.3.—Sketch of NASA LeRC 15 cm x 15 cm SWT.

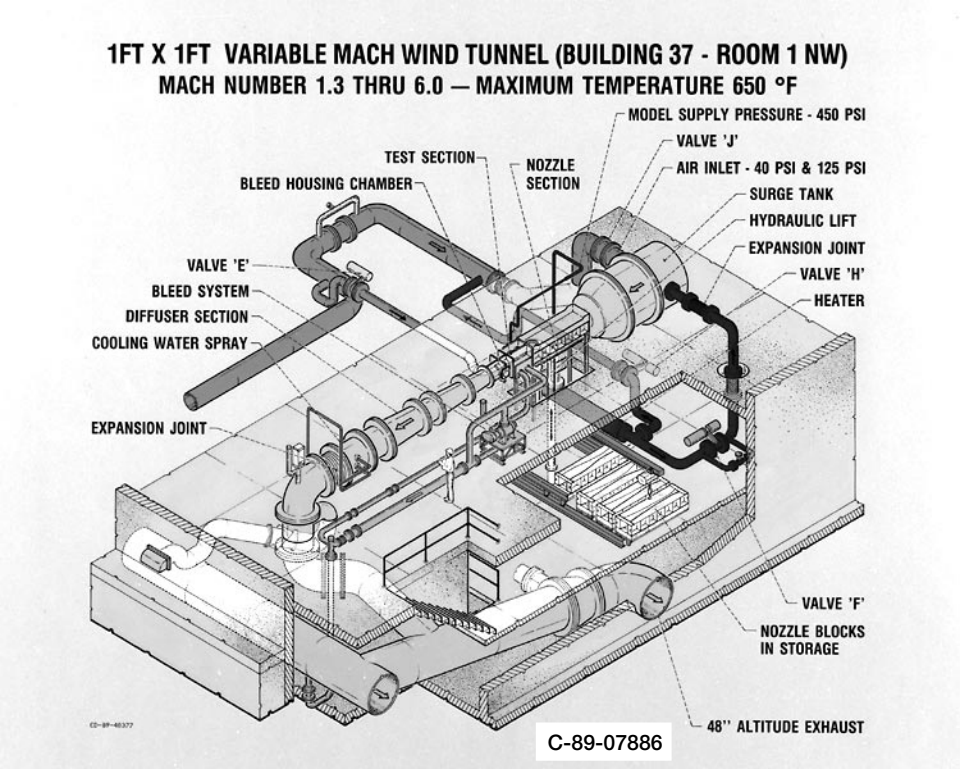

Figure 2.4.—Sketch of NASA LeRC 1 ft x 1 ft SWT.

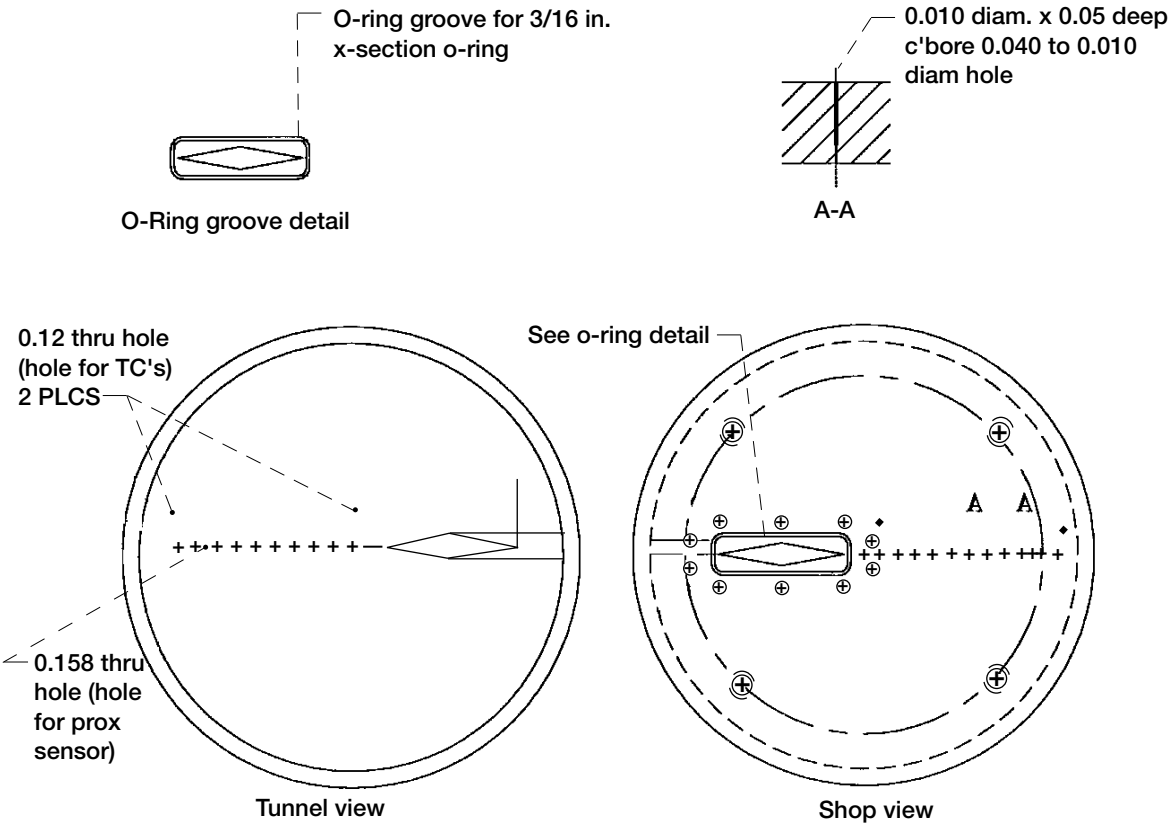

Figure 2.5.—Blueprint of insert plate.

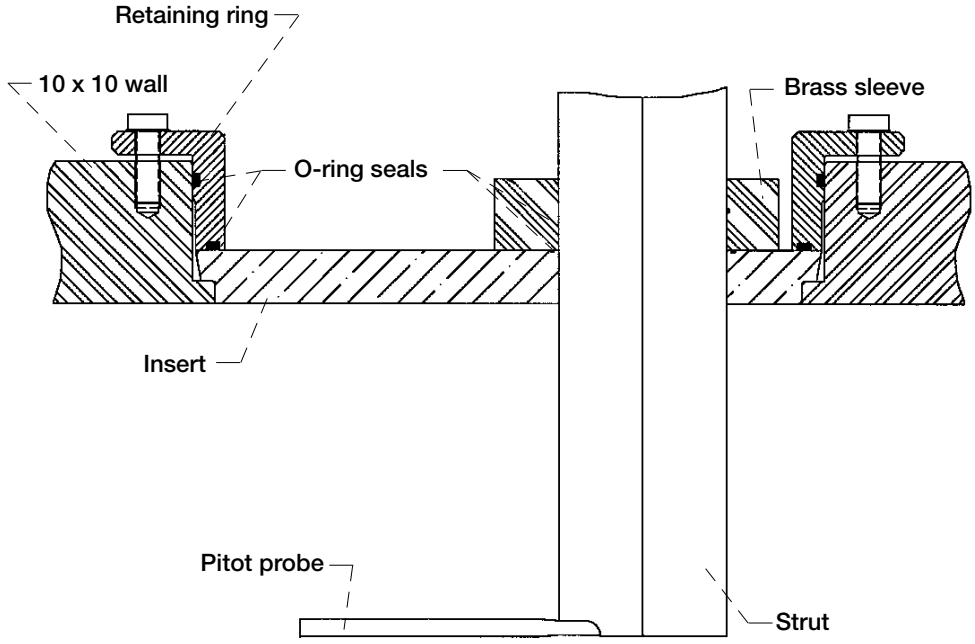

Figure 2.6.—Cut-away drawing of installed 10 ft x 10 ft hardware.

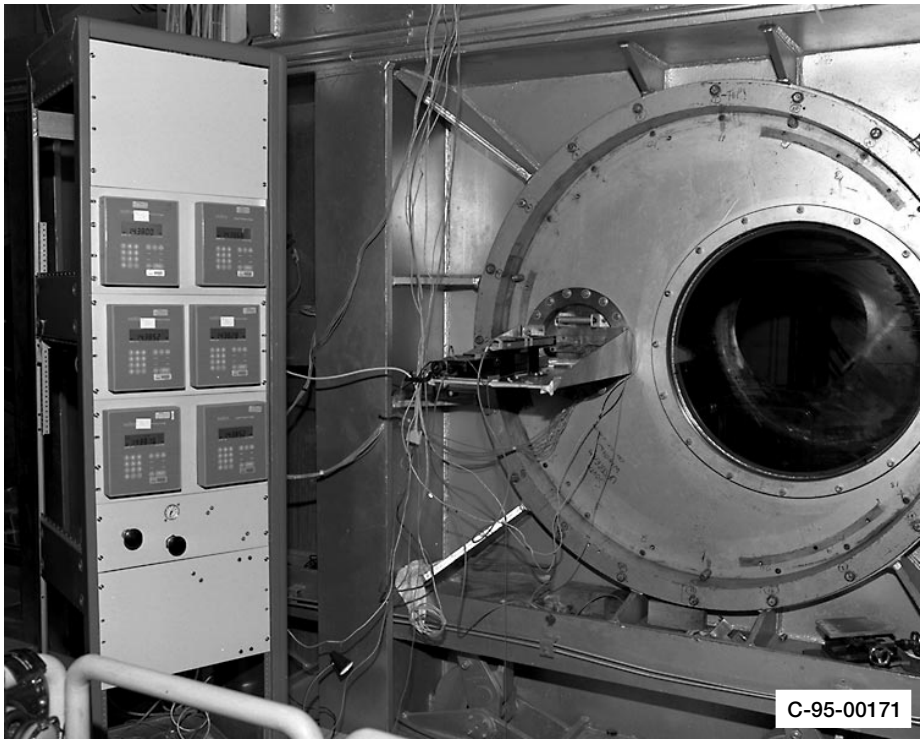

Figure 2.7.—Far view of test hardware outside of 10 ft x 10 ft SWT test section.

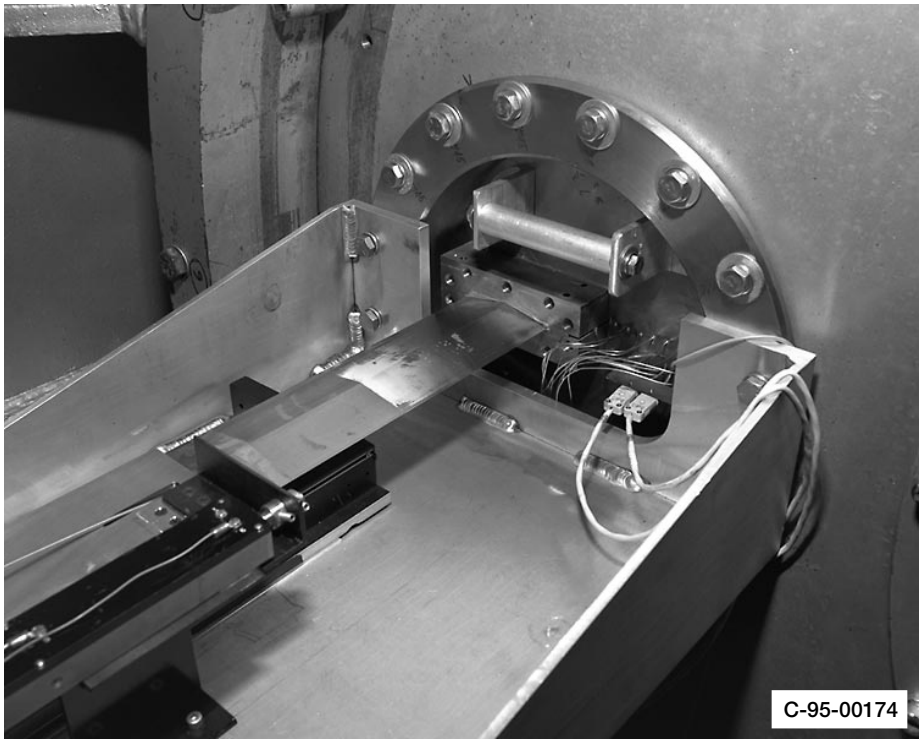

Figure 2.8.—Close-up view of test hardware on support table.

Figure 2.9.—Photograph of 10 ft x 10 ft SWT research pitot probes.

Figure 2.10.—Photograph of pitot probe leading edges.

Figure 2.11.—Photograph of diameter = 0.051 cm pitot probe.

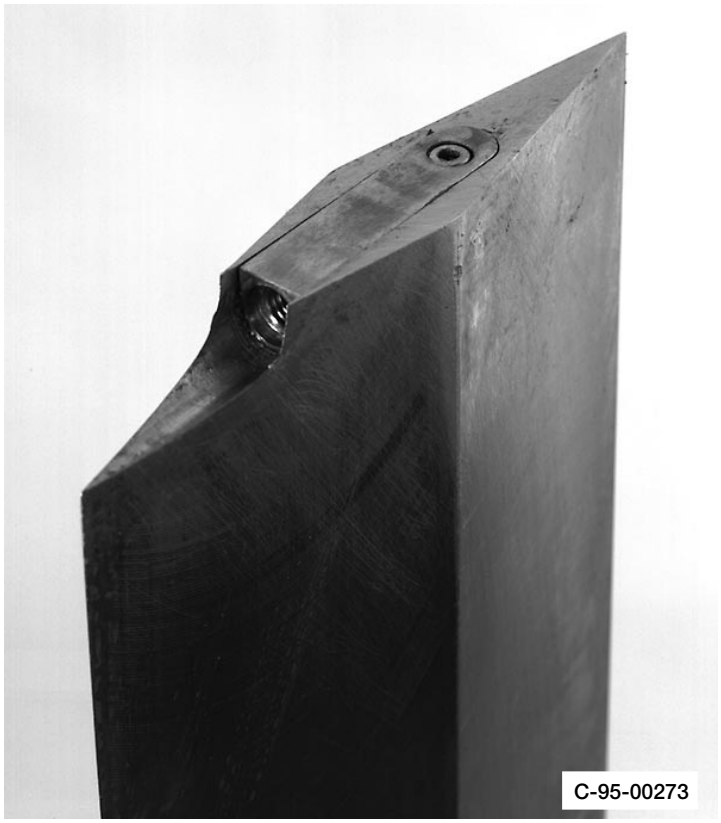

Figure 2.12.—Photograph of adapter piece installed in research strut.

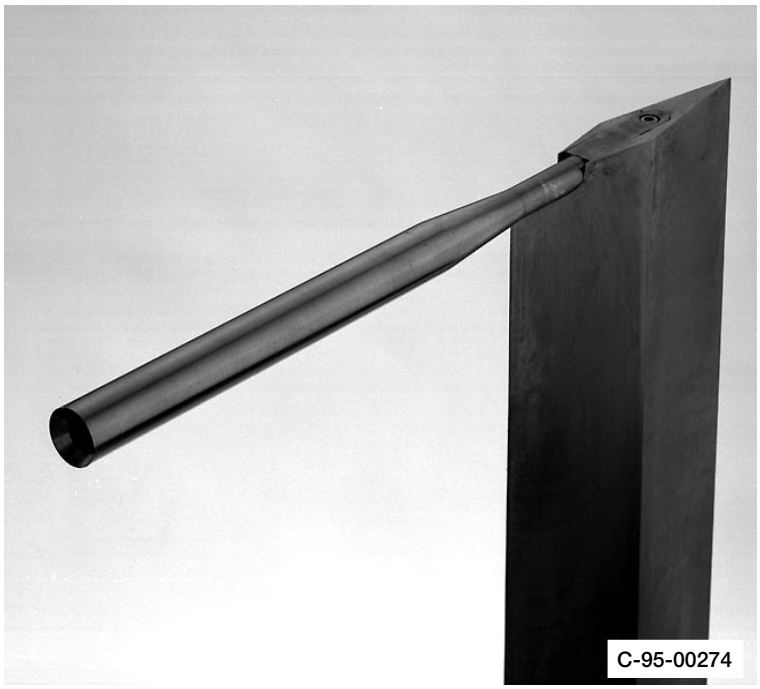

Figure 2.13.—Photograph of D = 1.27 cm pitot probe installed in research strut.

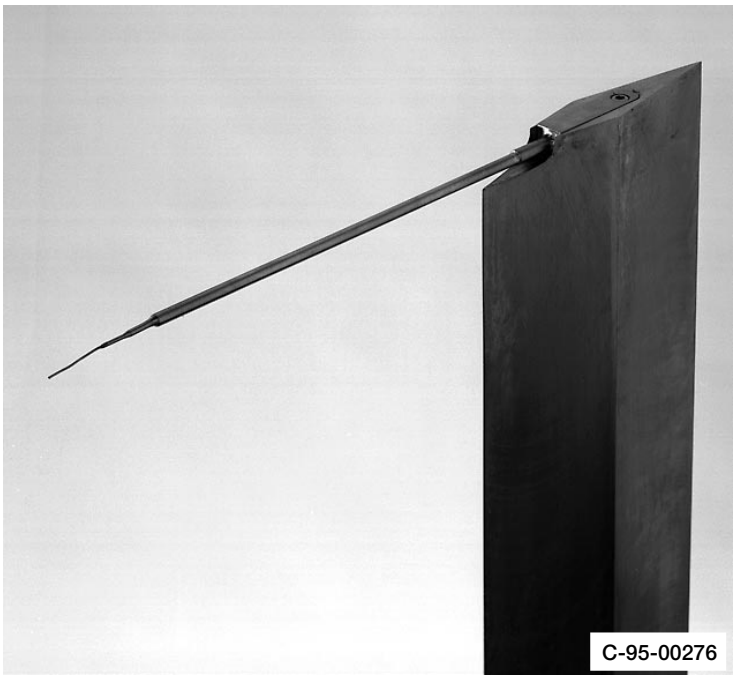

Figure 2.14.—Photograph of D = 0.051 cm probe installed in research strut.

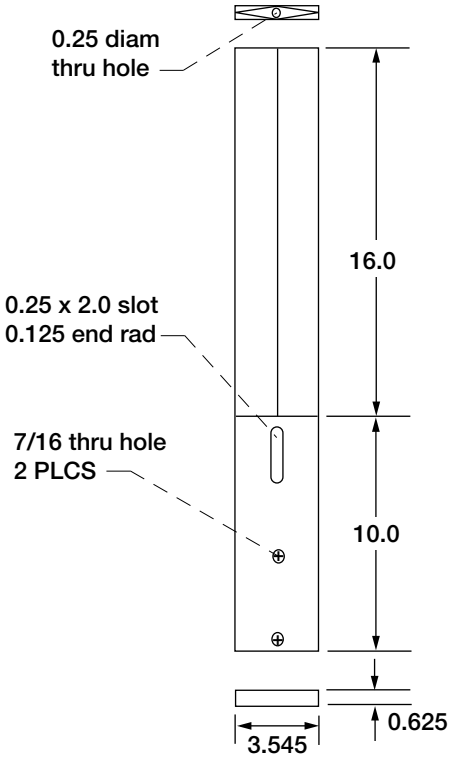

Figure 2.15.—Blueprint of research strut.

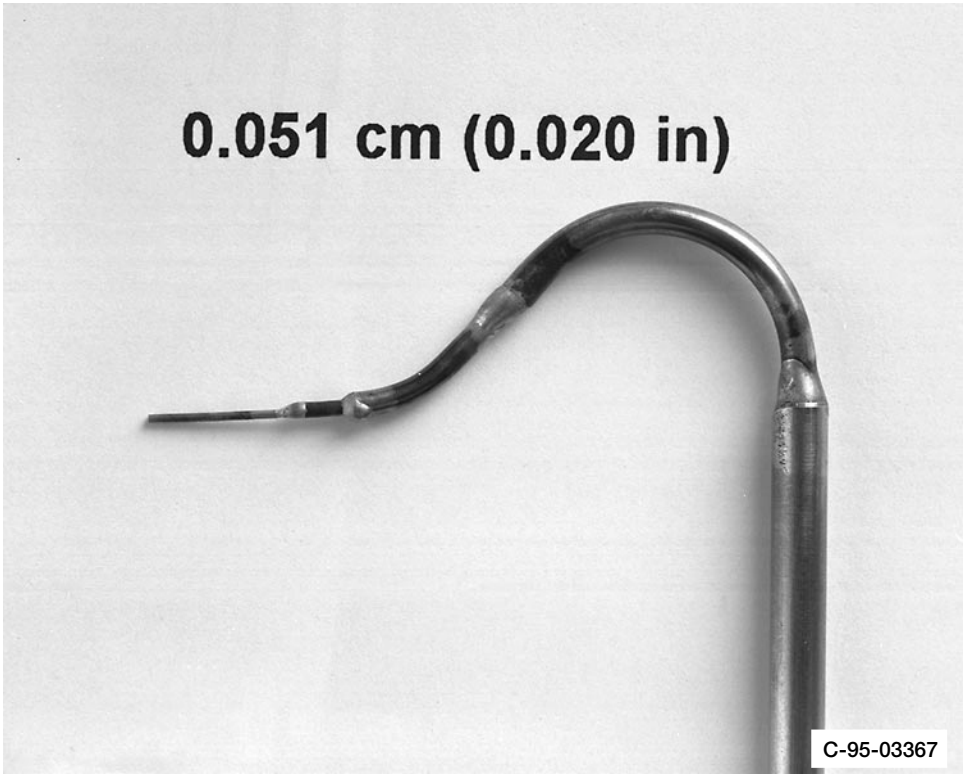

Figure 2.16.—Example of pitot probe used in 15 cm x 15 cm SWT and 1 ft x 1 ft SWT.

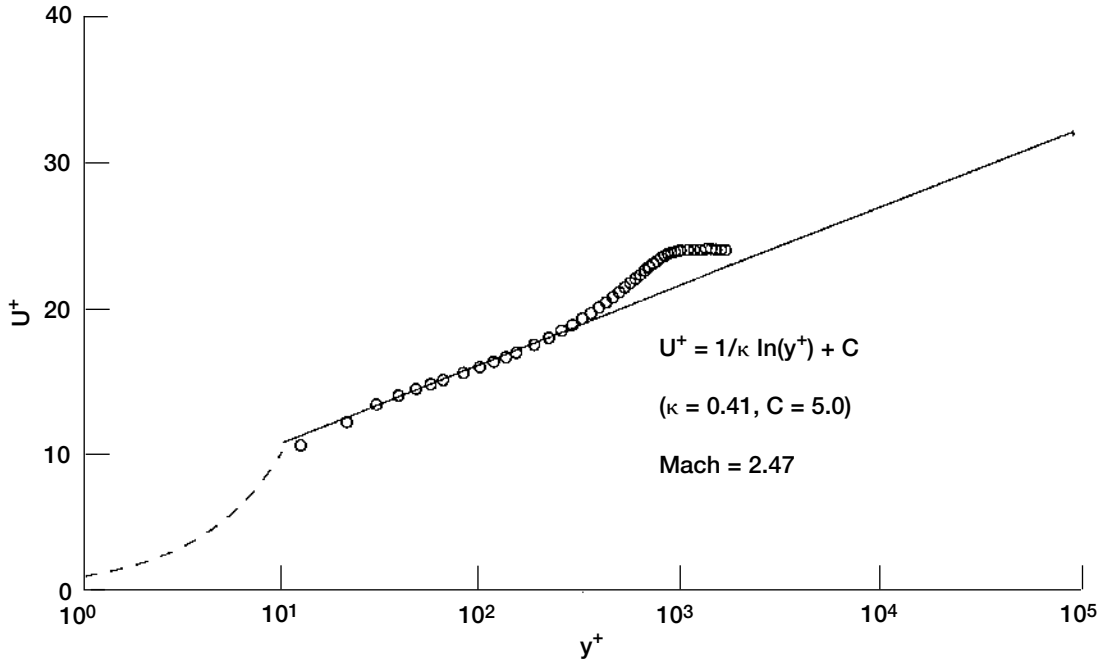

Figure 4.1.—Example of law of the wall profiles.

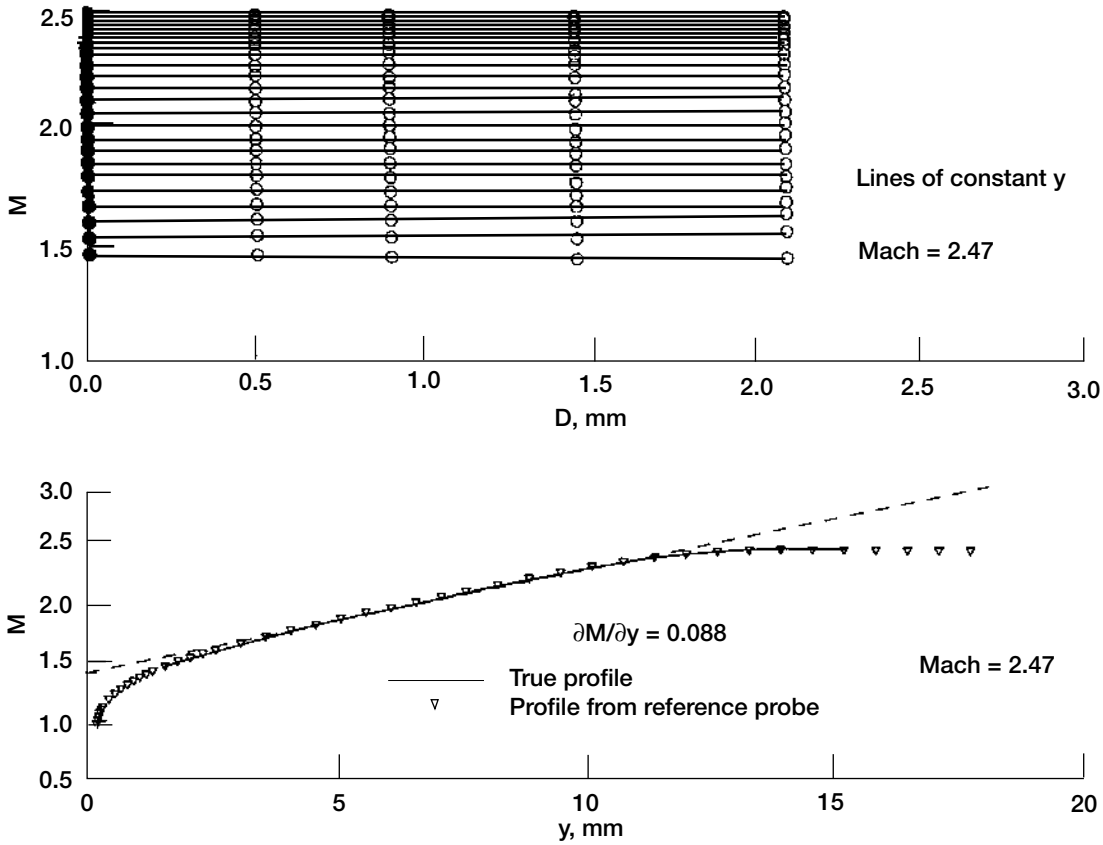

Figure 4.2.—Example of calculation of true Mach number, M_o.

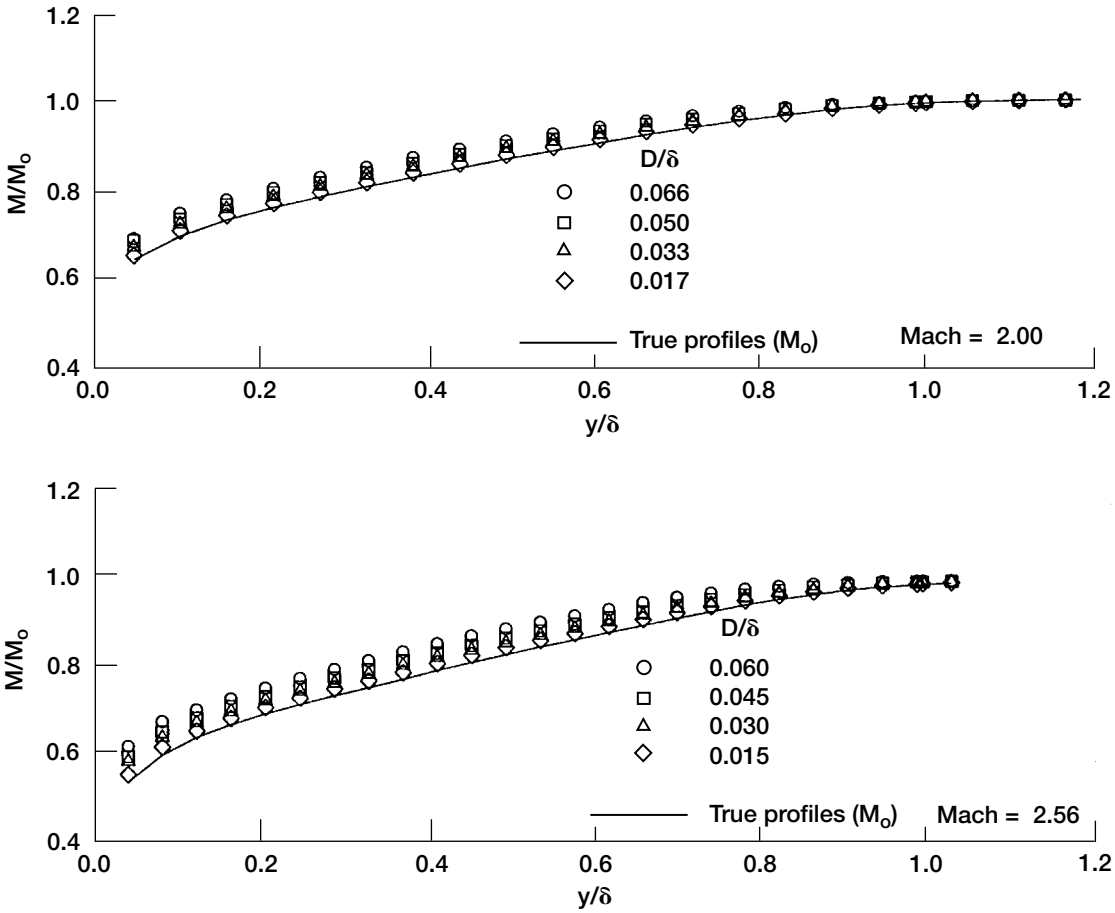

Figure 4.3.—Example of comparison of true and measured Mach profiles.

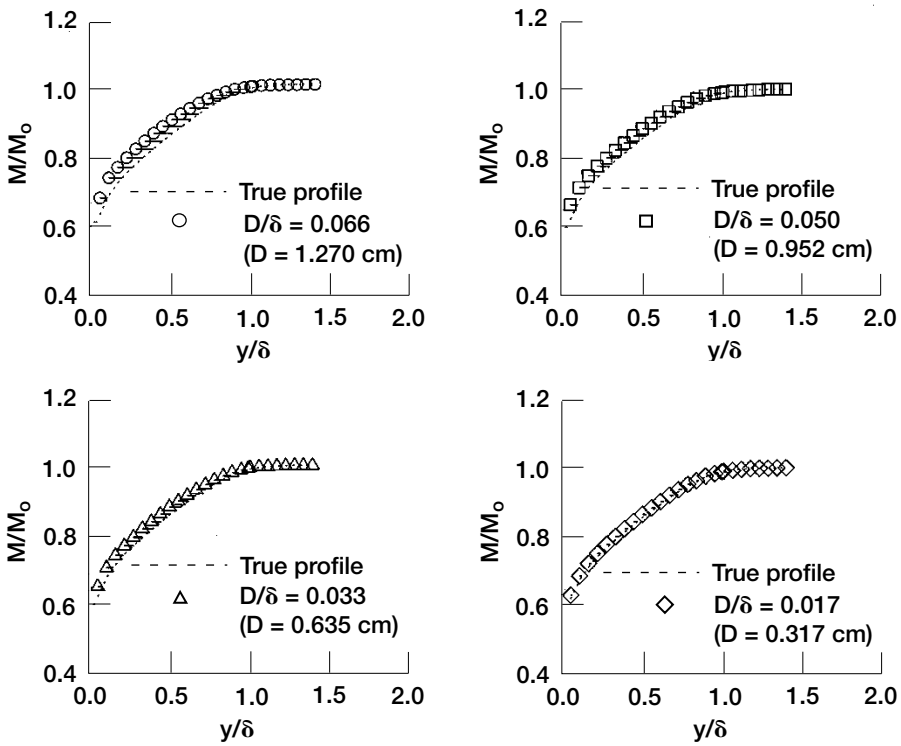

Figure 4.4.—Example of calculation of pitot probe centerline offset errors.

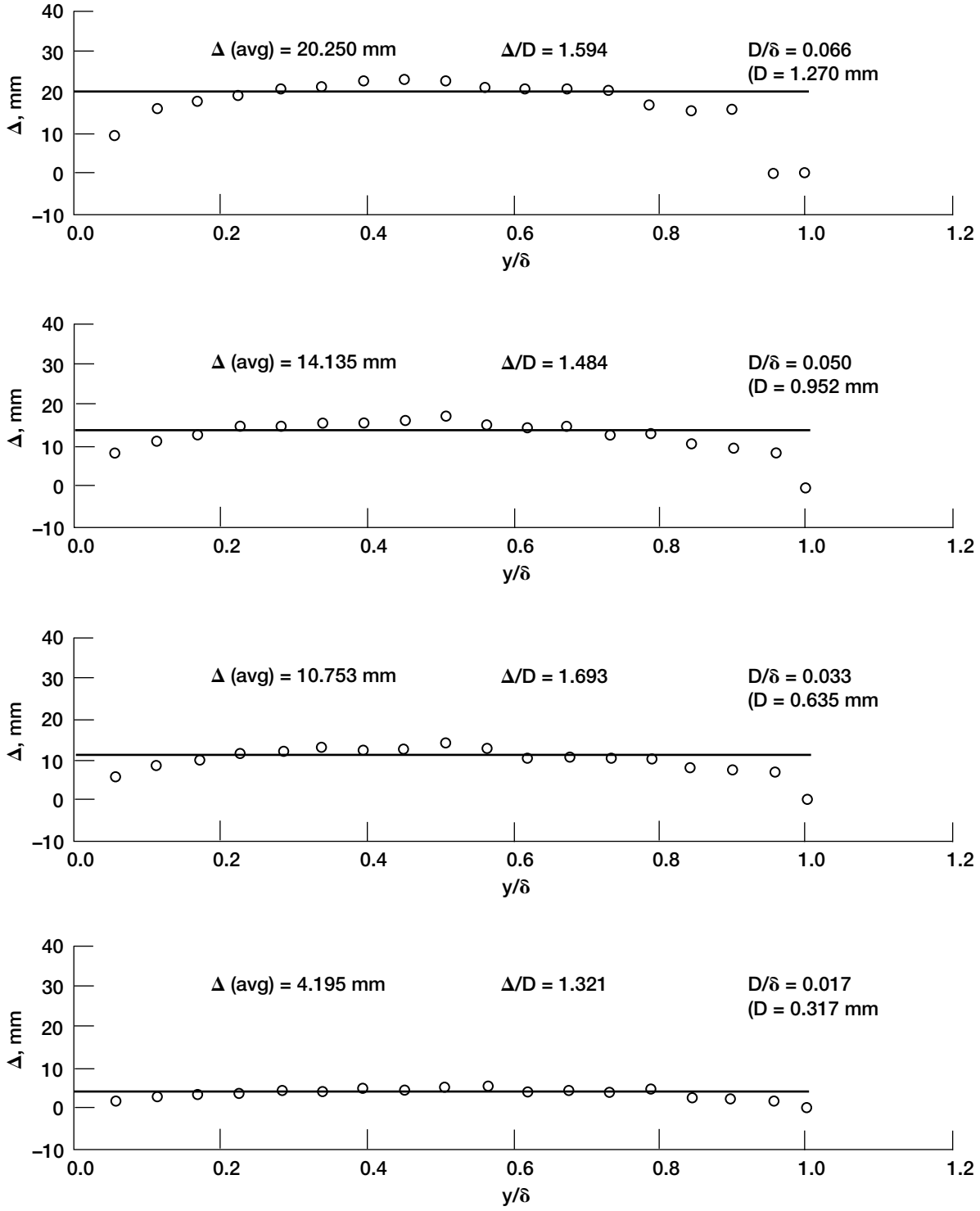

Figure 4.5.—Example of calculation of average Δ.

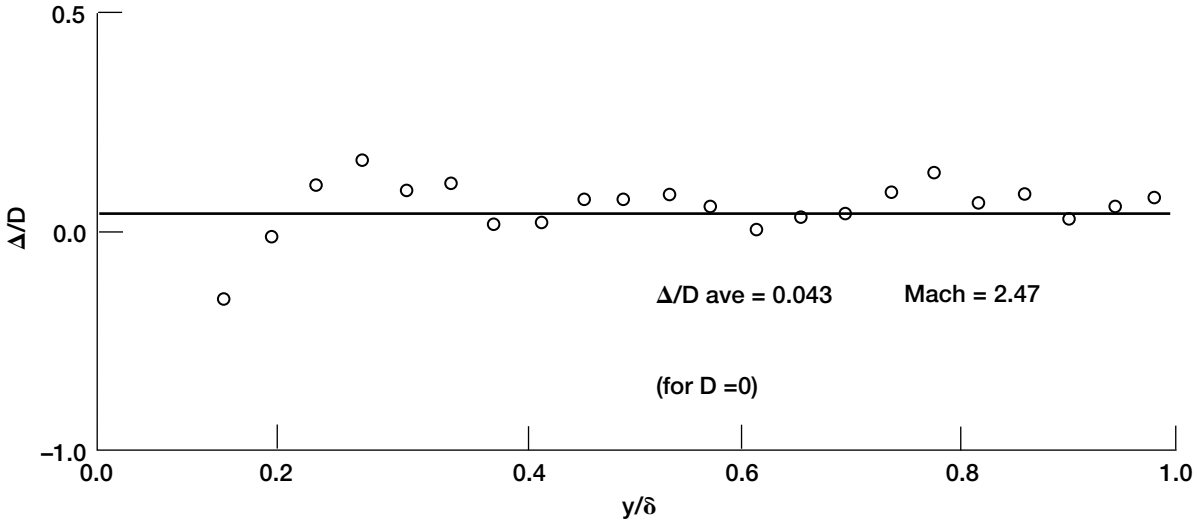

Figure 4.6.—Example of calculation of Δ at diameter = 0.

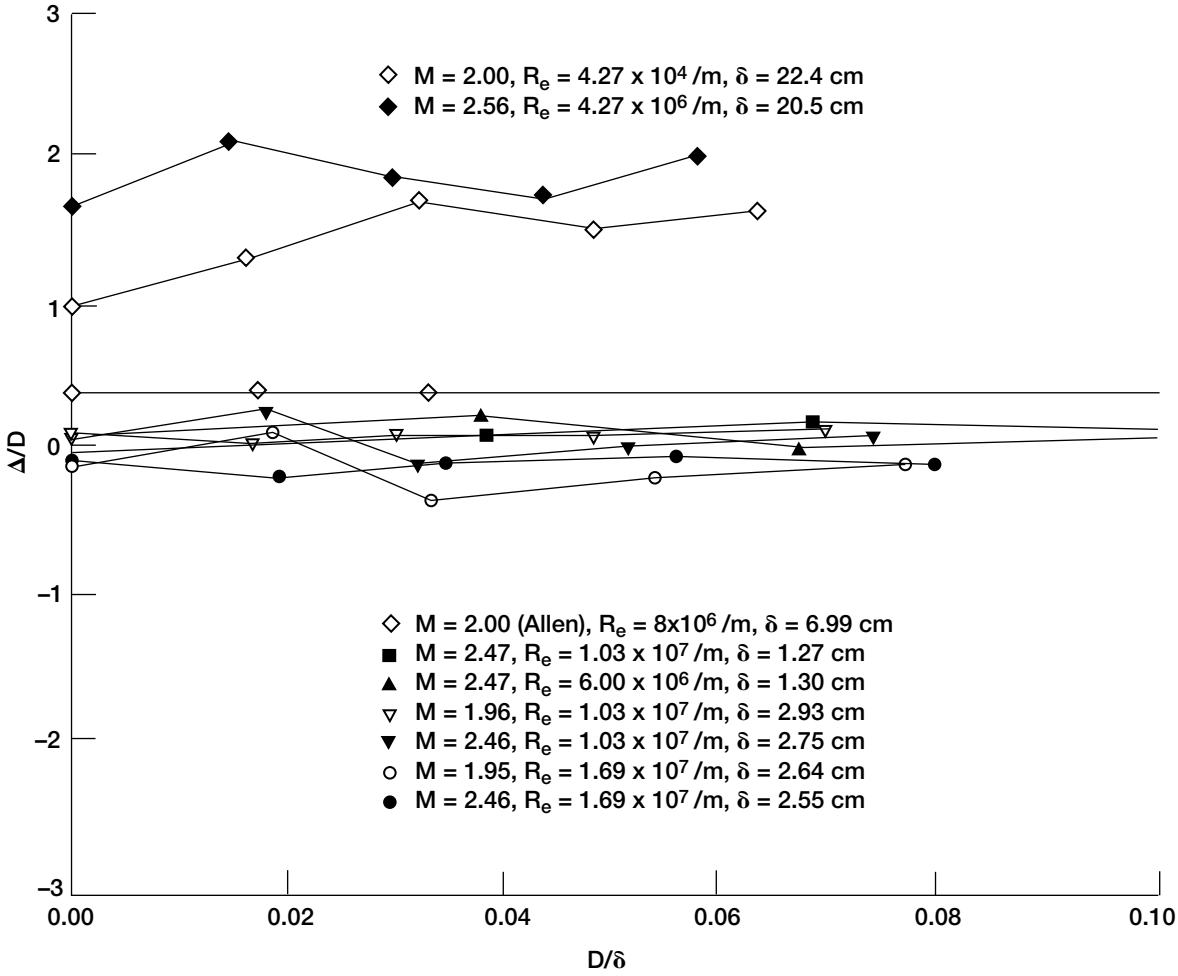

Figure 4.7.—Effect of probe size on displacement ratio in boundary layers.

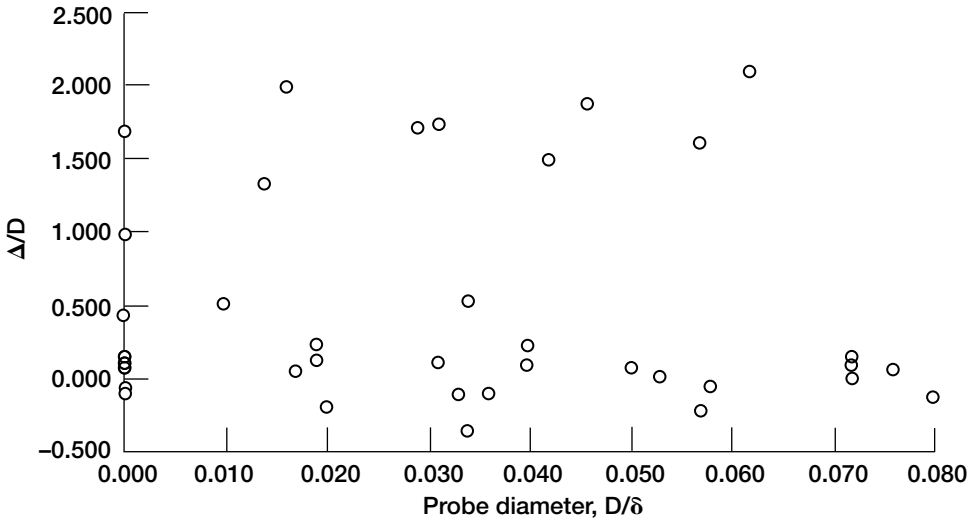

Figure 4.8.—Effect of probe diameter, D/δ, on centerline offset error.

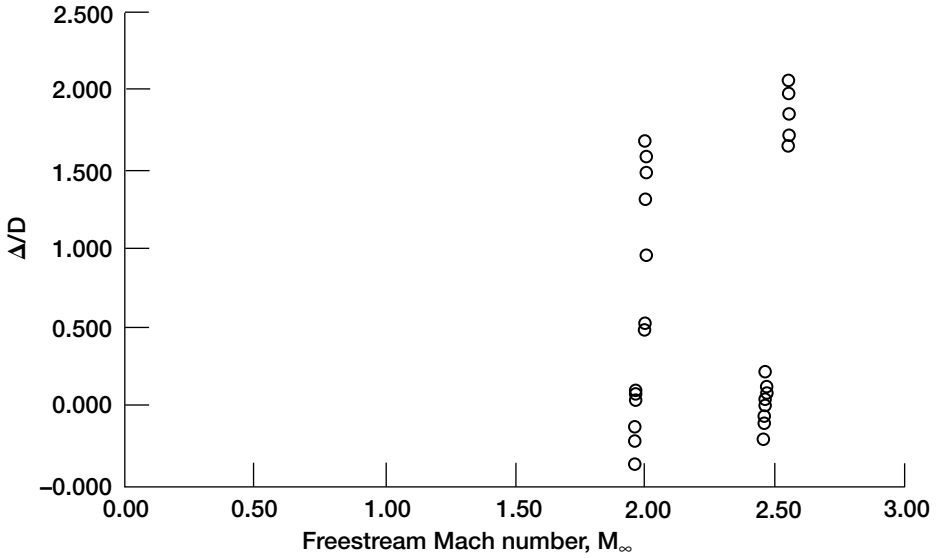

Figure 4.9.—Effect of freestream Mach number, M_∞, on centerline offset error.

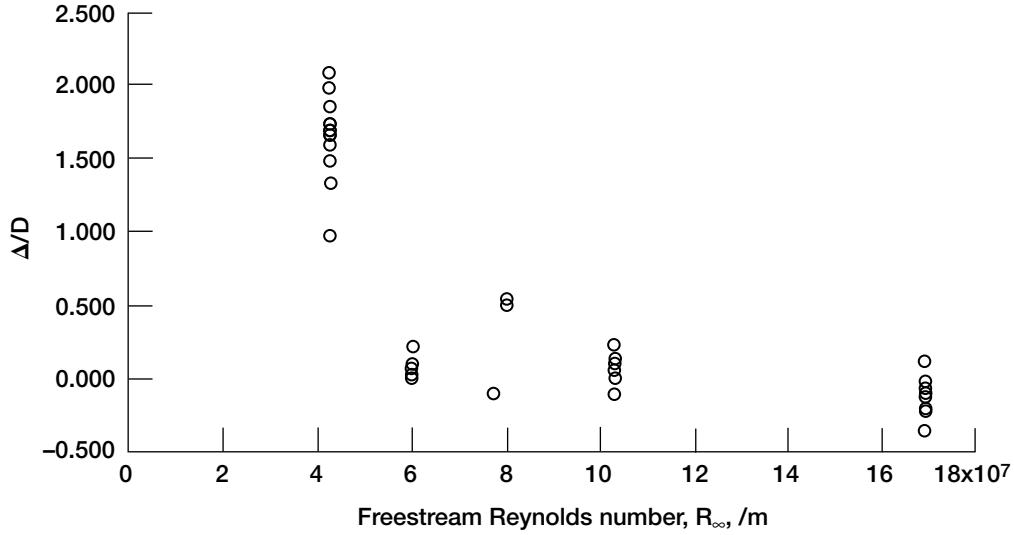

Figure 4.10.—Effect of freestream Reynolds number, R_∞, on centerline offset error.

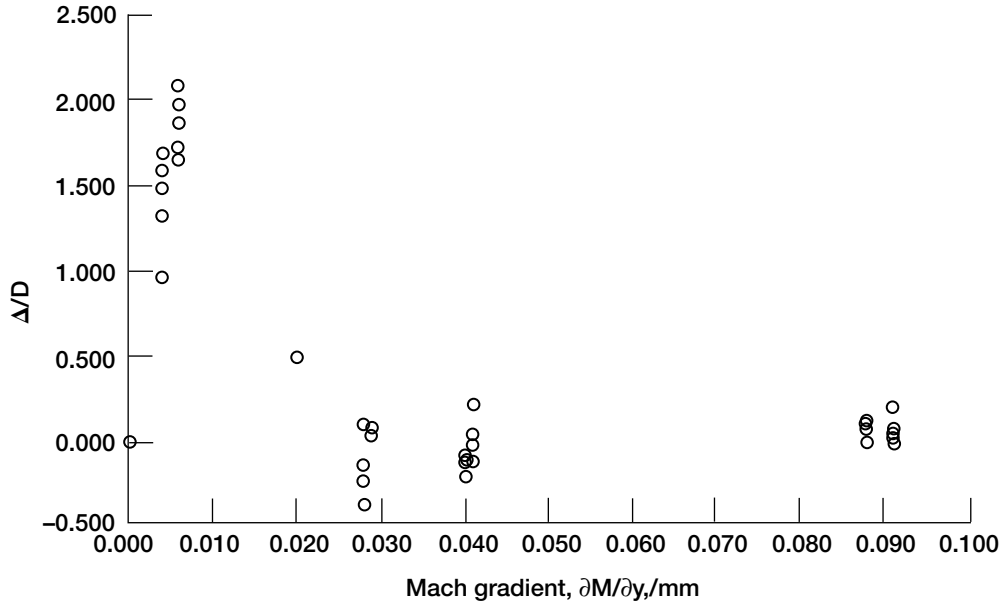

Figure 4.11.—Effect of Mach gradient, ∂M/∂y, on centerline offset error.

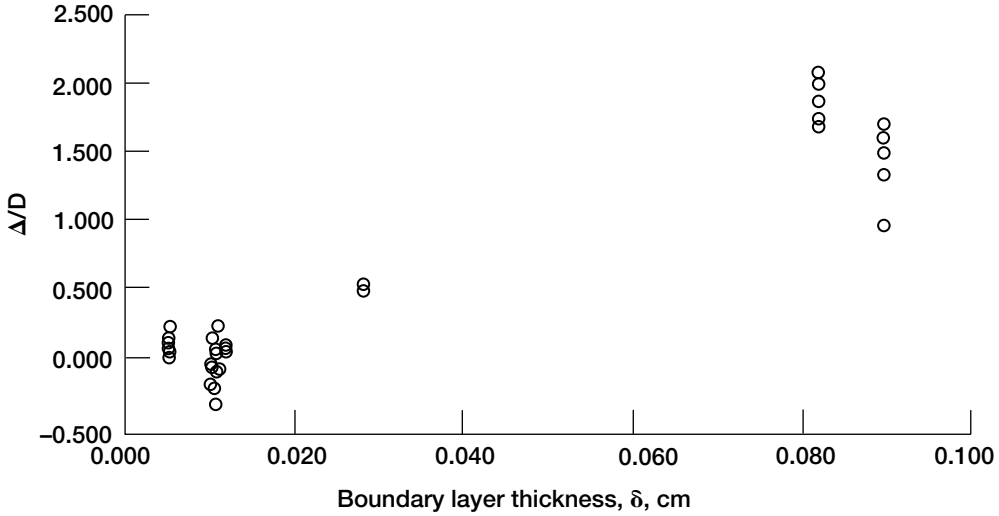

Figure 4.12.—Effect of boundary layer thickness, δ, on centerline offset error.

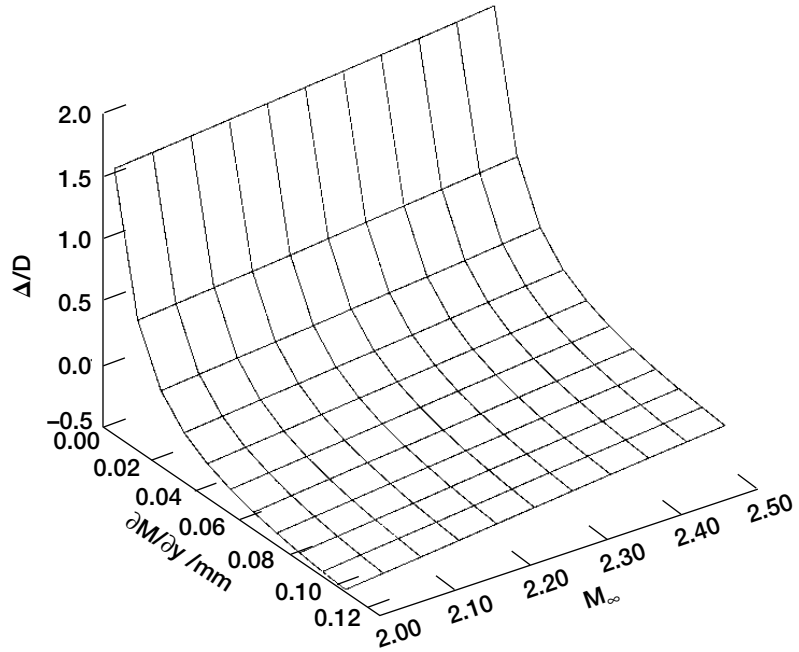

Figure 4.13.—3-Dimentional graph of Δ/D versus R_∞ and M_∞.

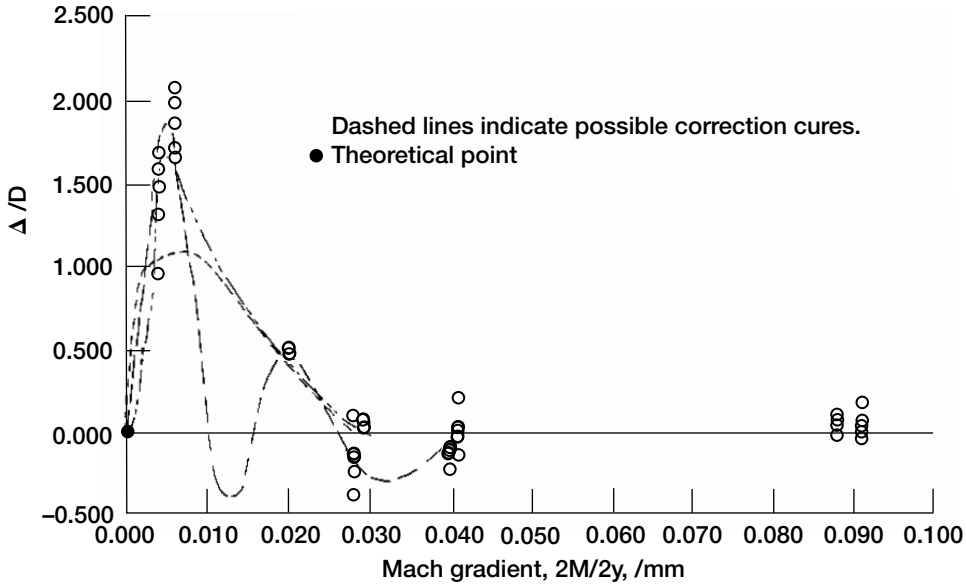

Figure 5.1.—Possible correction curves.

REPORT DOCUMENTATION PAGE

Form Approved
OMB No. 0704-0188

1. AGENCY USE ONLY (*Leave blank*)	2. REPORT DATE	3. REPORT TYPE AND DATES COVERED
	January 1997	Technical Memorandum

4. TITLE AND SUBTITLE

Factors Influencing Pitot Probe Centerline Displacement in a Turbulent Supersonic Boundary Layer

5. FUNDING NUMBERS

WU–505–62–52

6. AUTHOR(S)

Wendy I. Grosser

7. PERFORMING ORGANIZATION NAME(S) AND ADDRESS(ES)

National Aeronautics and Space Administration
Lewis Research Center
Cleveland, Ohio 44135–3191

8. PERFORMING ORGANIZATION REPORT NUMBER

E–10484

9. SPONSORING/MONITORING AGENCY NAME(S) AND ADDRESS(ES)

National Aeronautics and Space Administration
Washington, D.C. 20546–0001

10. SPONSORING/MONITORING AGENCY REPORT NUMBER

NASA TM–107341

11. SUPPLEMENTARY NOTES

This report was submitted as a dissertation in partial fulfillment of the requirements for the degree Bachelor of Science in Aerospace Engineering to the University of Minnesota in Minneapolis, Minneapolis, Minnesota 55455–0110. Responsible person, Wendy I. Grosser, organization code 2830, (216) 433–8680.

12a. DISTRIBUTION/AVAILABILITY STATEMENT

Unclassified - Unlimited
Subject Category 35

This publication is available from the NASA Center for AeroSpace Information, (301) 621–0390.

12b. DISTRIBUTION CODE

13. ABSTRACT ***(Maximum 200 words)***

When a total pressure probe is used for measuring flows with transverse total pressure gradients, a displacement of the effective center of the probe is observed (designated Δ). While this phenomenon is well documented in incompressible flow and supersonic laminar flow, there is insufficient information concerning supersonic turbulent flow. In this study, three NASA Lewis Research Center Supersonic Wind Tunnels (SWT's) were used to investigate pitot probe centerline displacement in supersonic turbulent boundary layers. The relationship between test conditions and pitot probe centerline displacement error was to be determined. For this investigation, ten circular probes with diameter-to- boundary layer ratios (D/δ) ranging from 0.015 to 0.256 were tested in the 10 ft x 10 ft SWT, the 15 cm x 15 cm SWT, and the 1 ft x 1 ft SWT. Reynolds numbers of 4.27×10^6 /m, 6.00×10^6 /m, 10.33×10^6 /m, and 16.9×10^6 /m were tested at nominal Mach numbers of 2.0 and 2.5. Boundary layer thicknesses for the three tunnels were approximately 200 mm, 13 mm, and 30 mm, respectively. Initial results indicate that boundary layer thickness, δ, and probe diameter, D/δ play a minimal role in pitot probe centerline offset error, Δ/D. It appears that the Mach gradient, $\partial M/\partial y$, is an important factor, though the exact relationship has not yet been determined. More data is needed to fill the map before a conclusion can be drawn with any certainty. This research provides valuable supersonic, turbulent boundary layer data from three supersonic wind tunnels with three very different boundary layers. It will prove a valuable stepping stone for future research into the factors influencing pitot probe centerline offset error.

14. SUBJECT TERMS	15. NUMBER OF PAGES
Turbulent boundary layer; Pitot probe displacement; Supersonic	48
	16. PRICE CODE: A03

17. SECURITY CLASSIFICATION OF REPORT	18. SECURITY CLASSIFICATION OF THIS PAGE	19. SECURITY CLASSIFICATION OF ABSTRACT	20. LIMITATION OF ABSTRACT
Unclassified	Unclassified	Unclassified	